

RE-491

SEGREGATION EFFECTS
DURING SOLIDIFICATION
IN WEIGHTLESS MELTS

(Interim Report)

August 1974

(NASA-CR-120721) - SEGREGATION EFFECTS DURING
SOLIDIFICATION IN WEIGHTLESS MELTS Interim
Report, 5 Jul. 1973 - 4 Jun. 1974 (Grumman
Aerospace Corp.) 68 p HC \$4.25 CSCL 22A

N75-20415

Unclas

G3/12 14689

RESEARCH DEPARTMENT



GRUMMAN AEROSPACE CORPORATION
BETHPAGE NEW YORK

SEGREGATION EFFECTS DURING SOLIDIFICATION
IN WEIGHTLESS MELTS

INTERIM REPORT

(Reporting Period: 5 July 1973 to 4 June 1974)

RE-491

by

Chou Li[†]

and

Morris Gershinsky[‡]

Research Department
Grumman Aerospace Corporation
Bethpage, New York 11714

Prepared in partial fulfillment of
Contract NAS 8-29662

for the

National Aeronautics and Space Administration
George C. Marshall Space Flight Center
Marshall Space Flight Center
Alabama 35812

August 1974

[†]Research Department, Grumman
Aerospace Corporation

[‡]Grumman Data Systems Corporation

Approved by: *Charles E. Mack, Jr.*
Charles E. Mack, Jr.
Director of Research

This report was prepared by Grumman Aerospace Corporation for the George C. Marshall Space Flight Center of the National Aeronautics and Space Administration in partial fulfillment of Contract NAS 8-29662. Our program on Segregation Effects in Weightless Melts has been partially supported by NASA/Marshall under the above contract.

TABLE OF CONTENTS

| <u>Item</u> | <u>Page</u> |
|---|-------------|
| Summary | 1 |
| Introduction | 3 |
| Review of Previous Contract | 5 |
| Importance of Evaporation | 9 |
| Computer Program without Surface Evaporation and Radiation | 13 |
| Mathematical Definition of Solidification Problem ... | 13 |
| Computer Program Developed under Present Contract | 19 |
| Generalized Solidification with Surface Evaporation | 21 |
| Evaporative Solidification of a Binary Alloy | 21 |
| Equations at the Evaporative Boundary | 22 |
| Start of Solidification | 24 |
| The Two-Boundary Problem-Derivative Estimation | 26 |
| Boundary and Mesh Points | 27 |
| Solution for Remaining Points | 28 |
| Convergence | 28 |
| Improved Computer Program | 31 |
| Use of Computer Program | 31 |
| Typical Computer Input | 39 |
| Computer Output | 41 |
| Representative Computed Results | 42 |
| Checking Program | 47 |
| Conclusions | 49 |
| Appendix I - Improved Computer Program | 51 |
| Appendix II - Glossary of Program Parameters | 61 |
| Appendix III - List of Symbols | 65 |
| References | 67 |

PRECEDING PAGE BLANK NOT FILMED

LIST OF ILLUSTRATIONS

| Figure | | Page |
|--------|---|------|
| 1 | Evaporation-Solidification of 0.01 Sb-Ge Initially at 970°C at 0.01 Second..... | 21 |
| 2 | Computed Temperature Distribution in the Semi- infinite Body at Different Times, t (initial grid spacing = 0.01 cm) | 44 |
| 3 | Computed Temperature Distribution in the Semi- infinite Body at Different Times, t (initial grid spacing = 0.001 cm) | 45 |
| 4 | Computed Temperature Distribution in the Semi- infinite Body at Different Times, t (initial grid spacing = 0.0001 cm) | 46 |

RECORDING PAGE BLANK NOT FILMED

ACKNOWLEDGMENT

The authors wish to thank Mr. R. C. Ruff of Marshall Space Flight Center for directing and monitoring this contract; they also wish to thank Dr. J. Bretz of NASA Headquarters in Washington, D.C. for helpful discussions.

PRECEDING PAGE BLANK NOT FILMED

SUMMARY

This report discusses the work partially supported under NASA Contract NAS 8-29662, "Segregation Effects During Solidification in Weightless Melts." The contract covers the period from July 5, 1973 to July 4, 1974.

During the contract period, the generalized problem of determining the temperature and solute concentration profiles during directional solidification of binary alloys with surface evaporation has been mathematically formulated. Realistic initial and boundary conditions have been defined, and a computer program has been developed and checked out.

The program computes the positions of two moving (evaporation and solidification) boundaries and their velocities of movement, and also the temperature and solute concentration profiles in the semi-infinite material body at selected instants of time.

The program has the following unique features:

- Two moving boundaries are involved, i.e., the evaporative boundary and freezing boundary
- Surface evaporation, and its related effects such as material loss, evaporative segregation, and surface cooling due to the heat of evaporation, have been considered
- Surface temperature is realistically determined by the combined effect of heat radiation, evaporative cooling, and thermal diffusion

- Material parameters such as solid and liquid densities, specific heats, thermal conductivities, mass diffusivities, and latent heat of fusion or evaporation, can all vary with both the temperature and composition
- Realistic phase diagrams involving curved liquidus and solidus lines are used

Our computer simulation work on solidification clearly shows that constitutional supercooling readily occurs and within-melt nucleation must then happen, particularly with reduced effective liquid mass transfer under zero-gravity conditions. Such results enabled us to explain and correlate some perplexing space solidification phenomena observed on Skylab, e.g., E. McKannan's weld (M551) and Prof. Adams' braze (M552) results (see Monthly Progress Reports Nos. 10 and 11). Detailed and quantitative application of the results of this computer program, however, still awaits the gathering of pertinent crystal growth data. A final report is expected to be written after these data are gathered and correlated.

INTRODUCTION

Space processing is moving closer to reality. Bigger, better, and more uniform single crystals of important semiconductors and welds or brazes of improved properties have already been made in space, as reported in the Third Space Processing Symposium at Marshall Space Flight Center. Although processing of structural materials may certainly have a profit potential in the long range, it appears that the high cost per pound of single-crystal electronic and optical materials makes these materials the most desirable contenders for immediate profitable returns from space processing. A selected single crystal study is, therefore, highly desirable to help us understand the segregation effects during solidification in weightless melts.

Important tools for understanding these segregation effects are analytic solutions or computer programs that simulate or predict what actually happens during space manufacturing. Such solutions and programs, furthermore, are probably necessary in space processing and other experiments where available time and experimental facilities are limited, the cost per sample or experiment is very high, and yet only a limited total number of tests or test samples can be conducted.

Theoretical predictions often greatly save time while computer simulation saves cost. Specifically, analytic solutions and computer programs allow us to answer many questions during the planning or execution of space experiments on material solidification, such as learning

- What phenomena are most important and what other phenomena are negligible

- Which influences are favorable to our understanding of weightless solidification and which are not
- What conditions lead to optimal combination of the favorable influences or elimination of the unfavorable ones
- What sample and processing conditions should be used
- What is the best way to analyze the resultant samples for understanding a particular phenomenon or influence
- How to save time and money — that is, how to maximize scientific return

We have developed a number of analytic solutions relating to solidification and evaporation (Refs. 1-3). Several important computer programs have also been developed. Some of these solutions and programs were developed under our Contract NAS 8-27891, and they are already proving useful in correlating actual experimental results (Refs. 4 and 5).

These analytic solutions and computer programs are, however, still in their early stages of development. The physical models involved are very simple and require considerable improvements to be used for other applications. It is, therefore, an important objective of this contract to refine and improve these models and the resultant analytic solutions and computer programs.

These refined solutions and programs are more widely useful, have greater predictive value, and provide more accurate results. Such accuracies are absolutely necessary to separate the rather subtle zero-gravity effects on solidification, in the presence of noise due to other unavoidable or unanticipated but ever-present

miscellaneous effects. As a result of this continued work, more efficient space experiments and greater scientific returns appear possible. More meaningful solidification experiments and fuller utilization of the unique space environment may also result.

The predicted results of our refined solutions and programs should, of course, first be checked with selected experiments. Another objective of this contract is, therefore, to design unique experiments to correlate the numerical results to actual solidification processes. This work is yet to be reported.

Review of Previous Contract

Under our NASA Contract NAS 8-27891, "Segregation Effects During Solidification in Weightless Melts" (Ref. 3), two types of melt segregation effects were studied: evaporative segregation, or segregation due to surface evaporation, and freezing segregation, or segregation due to liquid-solid phase transformation.

These segregation effects are closely related. In fact, evaporative segregation always precedes freezing segregation to some degree and must often be studied prior to performing meaningful solidification experiments. This is particularly true since evaporation may cause the melt composition, at least at the critical surface regions or layers, to be affected manyfold, often within seconds, so that at the surface region or layer the melting point and other thermophysical properties, nucleation characteristics, base for undercooling, and critical velocity to avoid constitutional supercooling, may be completely unexpected.

To predict the segregation effects of solidification time and temperature and to correlate these predictions with actual experimental data, "normal evaporation equations" were developed (Refs. 1, 4-6). An evaporative congruent temperature (or equi-evaporative

temperature) was then defined and listed for various binary or ternary alloys. Knowing these congruent temperatures and the solute and solvent evaporating rates, one can predict the type (solute depletion or enrichment) and magnitude of compositional or constitutional changes on the critical melt surface. One application of this unique temperature is to explain, predict, or plan "anomalous" evaporative or constitutional melting (on cooling) or solidification (on heating) experiments. We then computed for a simple model the reactive jetting forces due to surface evaporation and, in particular, showed that these forces can be very substantial on a differentially heated sample and may completely destroy the unique zero-gravity environment in space manufacturing (Ref. 7). In addition, these jetting forces may initiate surface deformation and vibration or other fluid disturbances, and may even produce some convection currents not normally anticipated. These studies also showed which sample materials are preferable, which should be avoided, and what impurities are harmful in producing excessive jetting or effective as stabilizing influences. The relationship between normal evaporation and normal freezing was then considered. Finally, applications of evaporation to space manufacturing concerning material loss and dimensional control, compositional changes, evaporative purification, surface cooling, materials standards, and freezing data interpretation were briefly described.

In the area of segregation due to solidification, we explained in some detail the normal freezing process and its successful use in the semiconductor industry. Various constitutional diagrams demonstrated the desirability of using nonconstant segregation coefficient techniques in metallurgical studies. We then stated the basic normal freezing differential equation, together with its

solutions for cases where the liquidus and solidus are quadratic, cubic, high-degree polynomial, and exponential functions of the melt temperature. The meaning of constant segregation coefficient was discussed, together with the associated errors due to curvatures of the liquidus and solidus lines and the best value of constant segregation coefficient for a given solidification experiment. Numerical methods for computing the normal freezing behavior were then given. Finally, as an example, the steady state solidification of the Ni-Sn system under conditions of limited liquid diffusion and nonconstant segregation coefficients was described. This system was studied in the M553 experiment on Skylab.

IMPORTANCE OF EVAPORATION

Evaporation is important in space melting and solidification for the following reasons:

- Significant evaporation of alloy components always occurs at high temperatures in space vacuum environments
- High-temperature evaporation of alloys is generally a neglected area of systematic research. Yet, unless the complete evaporative segregation behavior is understood and analyzed, solidification and its related segregation effects may not be properly studied because of ill-defined initial conditions. Before the liquid alloy can be controllably solidified or even melted, there is invariably some surface evaporation to cause changes in composition, freezing temperature, supercooling characteristics, nucleation and growth morphology conditions, and the like
- Controlled space evaporation probably most closely meets the requirements of our model of normal evaporation. We may thus be able to obtain material purity or evaporation standards, thermal properties, or even such basic thermodynamic properties as heat of evaporation, activity coefficients, and sticking coefficients that are difficult or impossible to obtain on earth

PRECEDING PAGE BLANK NOT FILMED

- Evaporation is a much simpler process than freezing, since the former does not involve such complicated phenomena as nucleation, phase transformation, and constitutional or nonconstitutional supercooling. Thus, in normal evaporation for specific geometries or alloy systems, we may ideally isolate and investigate such other phenomena as heat conduction or radiation, liquid or solid diffusion, fluid dynamics, and convection currents. Exact knowledge of these phenomena is necessary to understand solidification
- Evaporation causes surface cooling due to the heat of evaporation. This evaporative cooling effect is particularly important in low-melting materials (Ref. 8)
- Different rates of evaporation at various surface regions give rise to unbalanced forces and momenta that may produce erratic or unwanted accelerations, surface distortions and vibrations, exceedingly large "equivalent gravities," and possibly new types of powerful convection currents in zero-gravity conditions
- Evaporation may cause the surface composition of certain unwanted or unsuspected impurities to be increased a thousandfold or millionfold within seconds so that the layer's melting point and other thermophysical properties, nucleation characteristics, base for undercooling, and critical velocity to avoid constitutional supercooling may be completely

unexpected. In fact, anomalous "constitutional" or evaporative melting on cooling, or solidification on heating, is possible because of surface evaporation. In addition, very large artificial gravities (e.g., 10 g), strong fluid disturbances, or even new and significant convection currents may be produced from surface evaporation. These phenomena have been observed in the M553 movies, according to Dr. Martin Tobin of Westinghouse Co., Pa.

The much greater evaporative segregation effects, if unaccounted for, would almost certainly conceal any minor or subtle zero-gravity effects, particularly in the presence of other unknown or uncontrolled effects. Definitive space solidification work should probably, therefore, be preceded by an evaporative compatibility study of the sample materials and their possible associated impurities. In fact, evaporation is almost certain to be very important or so overwhelming that the effect of zero-gravity or freezing segregation may be masked or even reversed. A freely suspended molten drop in space may, for example, have its surface solute concentration greatly enriched (as much as a millionfold), by neglected and undetectable trace impurities within seconds of its deployment. We are then dealing at the critical surface layer with a completely new and unanticipated alloy having an entirely different composition, melting point, surface tension, thermophysical properties, latent heat of fusion, undercooling and nucleation characteristics, growth morphology, and the like.

From this we can also see that any analytical, numerical, or experimental study on solidification may yield completely unexpected or irrelevant results if the important and ever-present evaporation phenomena is not adequately taken care of. This is

particularly true in the study of nucleation, undercooling, and space manufacturing. Another important aspect of the present contractual work is to incorporate this generally neglected evaporation phenomena to define the exact initial and boundary conditions before and during the alloy solidification process.

COMPUTER PROGRAM WITHOUT SURFACE EVAPORATION AND RADIATION

Solidification, even in one-g, is a complicated process involving a multitude of interrelated phenomena such as mass and heat transfer, phase change, and fluid motion. Comprehensive reviews on solidification have been given, for example, by Chalmers (Ref. 9), Tiller (Ref. 10), Christian (Ref. 11), and Li (Ref. 12).

Solidification in zero-g is still very complicated. Here, gravitational force is negligibly small, but other effects as a result become important. For example, surface tension often plays a dominant role in determining the sample shape, processing technique and the resulting contamination level of the processed samples. Evaporation is another ever-present, complicating or dominating factor, but one that may be used to advantage when understood. Neglected, or improperly controlled evaporation may drastically change sample surface composition, fluid motion, equivalent gravities, nucleation, and undercooling characteristics as previously described. The previous program, under Contract NAS 8-27891, however, does not deal with evaporation.

Mathematical Definition of Solidification Problem

To understand thoroughly solute segregation either from combined evaporation and solidification, or in single-crystal growth, one requires a complete characterization of the (mass) diffusion and temperature fields in the solid crystal and remaining melt. The zero-gravity effect on the solidification may be overshadowed by other effects invariably present (such as evaporation) in any such growth process — a condition necessitating that such characterization be accurately defined. Unfortunately, the coupled partial differential equations for the diffusion and temperature

fields are generally not solvable. Although special case solutions have been given for some types of usually physically nonsatisfying, two-phase Stefan problems, for the general case solution we must resort to numerical computations. Existing numerical methods are always subject to such unrealistic assumptions as constancy of interfacial velocity, temperature or temperature gradients, segregation coefficients, diffusion constants, and other material thermophysical properties.

Under NAS 8-27891, a number of computer programs were developed to study the unidirectional solidification of a binary alloy. These programs employ analytical and numerical methods. The analytic program is based on some closed-form solutions of a simple model and gives results for our numerical program to compare. The model for the analytic program deals with a binary alloy at a constant temperature and concentration throughout the initial liquid melt, with the surface temperature instantaneously dropped below the liquidus temperature. The liquid-solid interface temperature is assumed constant, and the concentrations of the alloy at the interface are given by the phase diagram having curved liquidus and solidus lines. In addition, the interface boundary plane moves according to a square root law relative to the solidification time. The program also allows the interface temperature and interface boundary to vary from these fixed rules, but in practice the variation is negligible and not above the computer error level (Ref. 3).

Although covered in detail in the final report on NAS 8-27891, the mathematical formulation of the model is presented below for the sake of completeness.

We deal in unidirectional solidification with a liquid binary alloy to be directionally solidified into two phases, liquid and

solid. We consider the liquid alloy to be semi-infinite with original (at $t = 0$) temperature T_0 and concentration C_0 . Solidification occurs when the temperature at $x = 0$ is changed from T_0 to a lower value T_1 , either instantaneously or gradually, so that T_1 is below the temperature T_2 at which the liquid mixture at concentration C_0 can be in equilibrium with a solid phase. As solidification occurs, the solid phase grows and its boundary is located at $x = y(t)$, and the interface temperature at this point is $T_i(t)$. The partial differential equations describing the solidification process are the following:

$$a_s^2 \frac{\partial^2 T_s}{\partial x^2} = \frac{\partial T_s}{\partial t}, \quad D_s \frac{\partial^2 C_s}{\partial x^2} = \frac{\partial C_s}{\partial t} \quad \text{for } 0 < x < y(t) \quad (1)$$

$$a_\ell^2 \frac{\partial^2 T_\ell}{\partial x^2} = \frac{\partial T_\ell}{\partial t}, \quad D_\ell \frac{\partial^2 C_\ell}{\partial x^2} = \frac{\partial C_\ell}{\partial t} \quad \text{for } y(t) < x < \infty \quad (2)$$

where the variables T, C represent the temperature and concentration (of solute in solvent) and the subscripts ℓ, s denote the liquid and solid phases, respectively. The thermal and mass diffusion coefficients a_s, a_ℓ, D_s, D_ℓ are assumed constant. The following conditions are usually assumed throughout:

$$(a) \quad T_\ell(x, 0) = T_0 \quad \text{and} \quad C_\ell(x, 0) = C_0$$

$$(b) \quad T_\ell(\infty, t) = T_0 \quad \text{and} \quad C_\ell(\infty, t) = C_0$$

$$(c) \quad T_s(y(t), t) = T_\ell(y(t), t) = T_i(t)$$

$$(d) \quad C_s(y(t), t) = f_s(T_i(t))$$

$$(e) \quad C_\ell(y(t), t) = f_\ell(T_i(t))$$

$$(f) \quad \rho \gamma \dot{y}(t) = k_s \frac{\partial T_s}{\partial x} - k_\ell \frac{\partial T_\ell}{\partial x} \quad \text{for } x = y(t)$$

$$(g) \quad \left[f_s(T_i(t)) - f_\ell(T_i(t)) \right] \dot{y}(t) = D_\ell \frac{\partial C_\ell}{\partial x} - D_s \frac{\partial C_s}{\partial x}$$

for $x = y(t)$

In many cases, it is also assumed

$$(h) \quad y(t) = \alpha \sqrt{t} \quad .$$

Equation (a) describes the condition that the original mixture is all liquid at temperature T_0 and concentration C_0 . Equation (b) is a consequence of the semi-infinite nature of the mixture so that at any time t , the portion near infinity is unchanged. Equation (c) assumes that at the solid-liquid interface plane there is an interface temperature $T_i(t)$ and that both the solid and liquid phases at $x = y(t)$ have this temperature. There is no discontinuity in temperature. Equations (d) and (e) state that the concentrations of solid and liquid at the interface are given by the solidus and liquidus curves, respectively, of the constitutional diagram for the alloy. Equation (f) connects the derivative of the moving boundary with the redistribution of temperature and Eq. (g) connects the same boundary with that of concentration. Equation (h) relates the position of the interface boundary to the solidification time t .

The conditions on $T_s(0, t)$ and $C_s(0, t)$ are not fixed in our discussion, and a number of alternatives are considered:

1. $T_s(0,t) = T_1(t)$ with $T_1(t)$ equal to a constant for all t ;

2. linear, $T_1(t) = T_o + t(T_1 - T_o)/s$ for $t < s$ and $T_1(t) = T_1$ for $t \geq s$;

3. exponential, $T_1(t) = T_1 + (T_o - T_1) e^{-t/s}$ so $T_1(0) = T_o$ and $T_1(\infty) = T_1$.

For $C_s(0,t)$ the conditions considered are $C_s(0,t) = C_1$ usually taken $C_s(T_2)$ or at times a condition conserving mass between 0 and ∞ .

The two approaches we have pursued may be designated as analytic and numerical. The numerical approach can be applied to all three conditions on temperature whereas the analytic approach holds only the case of constant temperature instantaneously applied. A variant of this analytic method to apply to linear varying temperature has been investigated.

An analytic solution to the coupled partial differential equations (1) and (2) subject to the initial and boundary conditions (a) through (g) has been given (Ref. 13). A numerical program has been designed for the analytic solution.

These numerical programs developed under NAS 8-27891 are based upon finite difference approximations of the partial and ordinary derivatives and involve a variable spacing (for improved computing efficiency). The programs have given acceptable results and compared well with the reference analytic solution, where comparable. The basic physical properties such as densities, diffusivities, specific heats, thermal conductivities, and heat of fusion have been held to be constant, and independent of temperatures and concentrations.

COMPUTER PROGRAM DEVELOPED UNDER PRESENT CONTRACT

Under the present contract, we have extended the programs to allow for reasonable variation of these physical properties. The approach that has first been taken is to base the values of these physical properties upon extrapolated values of temperature and concentration, and then to determine the values of temperature and concentration. The process is then repeated by re-evaluations of the physical properties. Other modifications of our original program are: 1) to store the physical properties for each of the mesh points and to employ the appropriate quantities at each step, and 2) to recheck the mass and heat diffusion equations to make certain that the constancy of these properties is not assumed.

An additional major program modification has been the inclusion of evaporation effects. This includes evaporation before solidification that is mathematically identical to the problem of simple solidification in binary alloys. After solidification starts, significant evaporation may still exist. We then have to deal with two moving (solid-gas and solid-liquid) boundaries located at $y(t)$ for evaporation and at $z(t)$ for solidification, as will be described.

Modification of the initial and boundary conditions a-h has also been made to make the problem more physically meaningful. One such modification is to include a surface heat radiative loss term involving T^4 . This term affects the convergence of the problem and creates the need for different algorithms. As reported previously, (Ref. 14), the surface cooling due to evaporation is negligible for many metallic systems such as nickel and iron alloys, or other higher melting materials, and has not been studied in detail under this contract.

PRECEDING PAGE BLANK NOT FILMED

To obtain solutions for realistic boundary conditions and to include the various mass transfer effects, numerical solutions of the partial differential equations of heat and mass transfer are required. We have again used the finite difference method to obtain the numerical solution.

The boundary conditions for surface temperature include radiation cooling as given by the Stefan-Boltzmann equation and also include evaporative cooling for both components of the alloy. Raoult's law has been assumed in determining the evaporation rates. At the interface it is assumed that the temperature and concentration relationships for each phase are given by the constitutional diagram for the alloy. The temperature dependence of the thermal and mass diffusion coefficients are allowed for each phase.

GENERALIZED SOLIDIFICATION WITH SURFACE EVAPORATION

Evaporative Solidification of a Binary Alloy

Given a semi-infinite binary alloy melt, initially at concentration C_0 and temperature T_0 , we consider the solidification of the alloy due to surface heat loss by evaporation and radiation (Fig. 1). There are two separate regimes to be considered. The first is concerned with temperature and concentration variations before solidification begins; the evaporation causes the original liquid-vapor boundary to change. Thus, we have a moving boundary problem. The second regime begins with the solidification which introduces a boundary between the freezing solid and remaining liquid phases whose compositions, we assume, follow the phase diagram, i.e., solidus and liquidus curve relations hold. Consequently, after solidification begins, there are two moving boundaries: one is the evaporative boundary and the other is the freezing or solidification boundary.

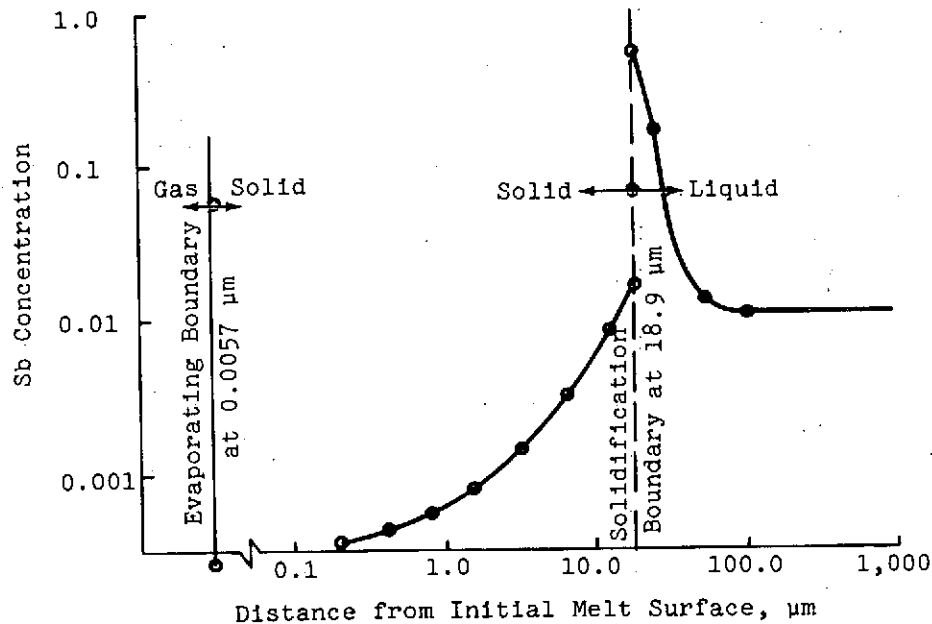


Fig. 1 Evaporation-Solidification of 0.01 Sb-Ge
Initially at 970°C at 0.01 Second

Equations at the Evaporative Boundary

We denote the evaporative boundary as $x = y(t)$ where $y(0) = 0$. The evaporation rates in $\text{mol/m}^2/\text{sec}$ for pure solute and solvent are, respectively (Ref. 15),

$$U = K_e 10^{A_u - B_u/T} (M_u T_s)^{-\frac{1}{2}}$$

$$V = K_e 10^{A_v - B_v/T} (M_v T_s)^{-\frac{1}{2}}$$

where $K_e = 5.83 \times 10^{-5}$, M_u , M_v are molecular weights for solute and solvent atoms, T_s is the evaporating surface temperature in degree K, and A_u , B_u , A_v , B_v are the evaporating constants for solute and solvent, respectively. If ρ_u and ρ_v are the solute and solvent densities, then

$$\frac{dy}{dt} = \frac{UM_u C}{\rho_u} + \frac{VM_v(1 - C)}{\rho_v}$$

where C is the concentration at the moving boundary.

The heat loss rate equation at the boundary due to radiation and evaporation is given by

$$\frac{\partial T}{\partial t} = -\epsilon \sigma T_s^4 - U\gamma_u C - V\gamma_v(1 - C)$$

where ϵ is emissivity coefficient, σ the Stefan-Boltzmann constant, and γ_u and γ_v are specific heats for solute and solvent, respectively.

The equation for the rate of concentration change is

$$\frac{\partial C}{\partial t} = - (U - V)C$$

Since the evaporative boundary is a moving one, and since both the evaporation temperature T and solute concentration C are functions of distance $x = y(t)$ and time t , i.e., $T = T(x,t)$ and $C = C(x,t)$, the total derivatives $\frac{dT}{dt}$ and $\frac{dC}{dt}$ may be obtained from the partials, i.e.,

$$\frac{dT}{dt} = \frac{\partial T}{\partial t} + \left(\frac{\partial T}{\partial x} \right)_{x=y} \left(\frac{dy}{dt} \right)$$

$$\frac{dC}{dt} = \frac{\partial C}{\partial t} + \left(\frac{\partial C}{\partial x} \right)_{x=y} \left(\frac{dy}{dt} \right)$$

where $\frac{\partial T}{\partial x}$ and $\frac{\partial C}{\partial x}$ are evaluated at the moving boundaries.

Given $\frac{dy}{dt}$, $\frac{dT}{dt}$, and $\frac{dC}{dt}$, we can integrate for y , T , and C for the moving boundary using a modified Euler method.

$$v_{t+\Delta t}^{(i)} = v_t + \Delta t \left(\frac{dv}{dt} \right)_t$$

$$v_{t+\Delta t}^{(i+1)} = v_t + \frac{\Delta t}{2} \left[\left(\frac{dv}{dt} \right)_t + \left(\frac{dv}{dt} \right)_{t+\Delta t}^{(i)} \right]$$

where $\frac{dv}{dt}^{(i)}$ is the value of the derivative at time $t + \Delta t$ using the value $v^{(i)}$ for v .

To determine $\frac{\partial T}{\partial x}$ at time t and $t + \Delta t$ requires knowledge of the distribution of temperatures at both times. Those at time $t + \Delta t$ are initially approximated by an extrapolation and are corrected using an approximated value of the temperature of the evaporating boundary with the heat diffusion difference equations. Since the change in temperature at the boundary is greatest due to the heat of evaporation, more iterations are applied to determine

it than to the determination of temperature distribution by means of diffusion equations. Similar considerations hold for the determination of $\frac{\partial C}{\partial x}$ and $\frac{dC}{dt}$.

The computations of the position of the evaporation boundary $[y = y(t)]$, temperature (T) , and solute concentration (C) at this boundary constitute an initial value problem in ordinary differential equations. Thus, given $y_0 = 0$, $T = T_0$, $C = C_0$, at time $t = 0$, and given also the equations for velocity of movement of this boundary dy/dt , and rate of change of temperature and solute concentration dT/dt , and dC/dt , we can determine for selected times the values of y , T , and C . The method used is an iterated Euler scheme:

$$y_{n+1} = y_n + \frac{\Delta t}{2} (y'_n + y'_{n+1})$$

where the initial value y'_{n+1} is taken as y'_n . This scheme must be connected to the problem of determining the temperature and solute concentration distribution within the semi-infinite body because the derivatives dy/dt , DT/dt , and dC/dt depend upon these quantities. The first step is to determine a first approximation of the temperature and solute concentration by extrapolation and then correct these values from the newly approximated values of the boundary position and the temperature and concentration thereat.

Start of Solidification

To determine the time when solidification has begun, the boundary temperature is compared with the temperature obtained by the inverse function for the liquidus curve evaluated at the boundary concentration. If the former is greater, then solidification has not yet begun. If it is smaller, then solidification has begun. In order to avoid an exact iterative procedure to determine the instant of solidification and to follow it up by a starting procedure for the first time interval thereafter, a simplified

approach has been taken that introduces a small error in the evaporative boundary and freezing boundary. By allowing the temperature to be below the solidification temperature by a small amount and by assuming that the temperatures at both boundaries are the same, a starting value of $x = z(t)$ of the freezing boundary is determined so that the loss in concentration due to solidification is compensated by the gain in concentration at the liquidus. Given the new temperature $TI2$ below the temperature at which solidification begins, we compute $CSS = FS(TI2)$ and $CLL = FL(TI2)$, the corresponding solid and liquid concentrations given by the phase diagram. To determine $DEL2 = ZI2 - YI2$, the distance between the evaporative boundary and solid-liquid interface, we assume that the solid is entirely at concentration CSS , and the liquid varies linearly from CLL to $CC(II2)$, the concentration at the first mesh point $x(II2)$ after the evaporative boundary. The total concentration is to equal the concentration in the whole regime had no solidification taken place. We assume it to be $CL2$ computed at $YI2$ and to vary linearly to $CC(II2)$ at $x(II2)$. This yields the equation

$$\begin{aligned} CSS * DELZ + (CLL + CC(II2))/2 * (x(II2) - YI2 - DELZ) \\ = (CL2 + CC(II2))/2 * (x(II2) - YI2) \end{aligned}$$

Hence

$$DELZ * [CSS - (CLL + CC(II2))/2] = (x(II2) - YI2) * (CL2 - CLL)/2$$

where

$$DELZ = (CLL - CL2)/2 * (x(II2) - YI2) \div (CLL + CC(II2))/2 - CSS$$

Then

$$ZI2 = YI2 + DELZ \quad \text{and} \quad \frac{dz}{dt} = \frac{DELZ}{DELTS}$$

This enables us to begin the next time step with initial values for $y(t_s)$, $z(t_s)$, $\frac{dy}{dt}$, $\frac{dz}{dt}$, $T(y(t_s)) = T(z(t_s)) = T_{I2}$, and $C(y(t_s)) = C_{SS}$, $C_s(z(t_s)) = C_{SS}$, $C_\ell(z(t_s)) = C_{LL}$.

The Two-Boundary Problem-Derivative Estimation

The equations at the freezing boundary are those given in the Grumman Final Report RE-458 to Contract NAS 8-27891 (Ref. 3), with the exception that the freezing boundary is now called $x = z(t)$ and not $x = y(t)$ as in Eq. 49 c-g. At every time step we must compute (in addition to the temperature and concentration at the evaporation boundary) the temperature at the freezing boundary. The concentrations are determined by the phase diagram. The method we employ is that which determines T (the solidification temperature) and $\frac{dz}{dt}$ by means of Eq. (49) f,g. Having obtained $\frac{dz}{dt}$ we obtain $z(t)$ by means of a modified Euler method. Since the Eq. (49) f,g required approximation for $(\frac{\partial T_s}{\partial x})_{z,t}$ and $(\frac{\partial C_s}{\partial x})_{z,t}$, we must develop techniques for these approximations appropriate to various situations for mesh points. In addition, for the computation of $\frac{dy}{dt}$, $\frac{dT}{dt}$, and $\frac{dC}{dt}$ at the evaporative boundary, we also need $(\frac{\partial T}{\partial x})_{y,t}$ and $(\frac{\partial C}{\partial x})_{y,t}$. When there are two mesh points between y and z , then the techniques alluded to above are available. This involves determining $\frac{\partial^2 T}{\partial x^2}$ at both y and z and the same for $\frac{\partial^2 C}{\partial x^2}$. When there is only one mesh point between y and z , then $\frac{\partial^2 T}{\partial x^2}$ at both points are the same. When there are no mesh points between y and z , then we can assume either that $\frac{\partial^2 T}{\partial x^2}$ is zero and hence $(\frac{\partial T}{\partial x})_y = (\frac{\partial T}{\partial x})_z = \frac{T(z) - T(y)}{z - y}$ or that

$$\frac{\partial^2 T}{\partial x^2} = k \frac{\partial T}{\partial x} \quad \text{and hence} \quad \left(\frac{\partial T}{\partial x}\right)_y = \left(1 - \frac{z-y}{2} k\right) \frac{\partial T}{\partial x} \quad \text{and}$$

$$\left(\frac{\partial T}{\partial x}\right)_z = \left(1 + \frac{z-y}{2} k\right) \frac{\partial T}{\partial x}. \quad \text{The choice of } k \text{ must be small so that}$$

$\frac{\partial^2 T}{\partial x^2} = k \frac{\partial^2 T}{\partial x^2} = k^2 \frac{\partial T}{\partial x}$ is negligible. Thus, since $z-y$ is also very small this option is indistinguishable from $\frac{\partial^2 T}{\partial x^2} = 0$. We

have three cases: 1) no mesh points between two boundaries and we assume $\frac{\partial^2 T}{\partial x^2} = 0$, $\left(\frac{\partial T}{\partial x}\right)_y = \left(\frac{\partial T}{\partial z}\right)_z$, 2) one mesh point between y and z when $\frac{\partial^2 T}{\partial x^2}$ is obtained from the three points and

$$\left(\frac{\partial T}{\partial x}\right)_y = \frac{T(z) - T(y)}{z - y} - \frac{(z - y)}{2} \frac{\partial^2 T}{\partial x^2} \quad \text{and} \quad \left(\frac{\partial T}{\partial x}\right)_z = \frac{T(z) - T(y)}{z - y} +$$

$$\frac{(z - y)}{2} \frac{\partial^2 T}{\partial x^2}, \quad \text{and} \quad 3) \text{ when two or more mesh points, say } x_i \text{ and}$$

x_{i+1} , are between y and z so that we can compute $\left(\frac{\partial^2 T}{\partial x^2}\right)_z$ and $\left(\frac{\partial^2 T}{\partial x^2}\right)_y$ separately and distinct. Then $\left(\frac{\partial T}{\partial x}\right)_y = \frac{T(x_i) - T(y)}{x_i - y} -$

$$\frac{(x_i - y)}{2} \left(\frac{\partial^2 T}{\partial x^2}\right)_y \quad \text{and} \quad \left(\frac{\partial T}{\partial x}\right)_z = \frac{T(z) - T(x_{i+1})}{z - x_{i+1}} + \frac{(z - x_{i+1})}{2} \left(\frac{\partial^2 T}{\partial x^2}\right)_z.$$

In general, it is necessary to compute $\frac{\partial^2 T}{\partial x^2}$ and $\frac{\partial^2 C}{\partial x^2}$ in three

ways, two ways indicated above for the solid regime and a third for the liquid side of the freezing boundary. It is similarly necessary to compute $\frac{\partial T}{\partial x}$ and $\frac{\partial C}{\partial x}$ in three ways.

Boundary and Mesh Points

When boundary points come close to mesh points, the computation of derivatives may be vitiated by closeness to mesh point.

Therefore, tests are made to determine when such closeness occurs as usually expressed in terms of a decimal fraction of the interval. In that case, the reference point is moved to the next mesh point and the values of T and C at the skipped mesh point are obtained by linear interpolation. This interpolation depends on which side of the solid-liquid interface the mesh point lies. For the evaporative boundary similar considerations hold.

Solution for Remaining Points

The solution for the remaining points is obtained as in the Final Report previously mentioned, pages 3-14 and 3-15 (Ref. 3). One change is, however, necessary because the first mesh point (or more) are no longer under consideration if the evaporative boundary has passed them. The subroutine TRIST is used to solve for the remaining points. In this subroutine we compute the values of temperature and concentration at intermediate mesh points when given the values at the two extreme mesh points. We replace the values at the mesh point to the left of the evaporative boundary by those at the evaporative boundary point, before solving for the intermediate points. This can be done without destroying any useful information since that mesh point is no longer used in the computations. The subroutine TRIST does not depend upon equal spacing or any regular spacing and therefore can accommodate this usage.

Convergence

The convergence problem is the crux of the program. Oscillation tends to cause the needed quantities to overflow. Thus, tests must be made on all the quantities to contain them within reasonable bounds. The subroutine MOTON is used to check the monotonicity of these consecutive points. In addition, the temperature at the evaporative boundary is necessarily less than the temperature at

the freezing boundary. This condition is always imposed in the program.

In addition, the solution for the solidification temperature and freezing boundary derivative (especially the latter) involves very rapidly changing quantities. More iterations should, therefore, be expended in this part of the program. Fewer iterations are needed for determining the evaporative boundary, and the temperature and concentration at that boundary. The program allows five iterations in the former for each of the latter. The number of iterations of the latter is used in a manner analogous to that described in Final Report RE-458 (Ref. 3).

An input quantity NIT (usually a multiple of 4) gives the maximum number of iterations. When $NIT/2$ iterations occur and convergence is not reached, the time step size is halved. This process is continued until either convergence is attained or the minimum step allowed by the program has been iterated $NIT + 1$ times. In this case the program may stop or continue on using the nonconverged quantities. Very often these quantities are sufficiently smooth so that convergence will occur on the next interval and the program gives satisfactory results.

However, if the program proceeds with the minimum step and the maximum number of iterations, the results may be spurious. In case of overflow, there is no doubt of it. Otherwise the user must look at results to decide whether he finds them reasonable.

IMPROVED COMPUTER PROGRAM

The complete computer program for the generalized solidification problem is listed herein (see appendix), together with a glossary explaining the special names used in the program. This computer program has the following unique features:

- Surface evaporation, and its related effects such as material loss, evaporative segregation, and surface cooling due to the heat of evaporation, have been considered
- Material parameters such as solid and liquid densities, specific heats, thermal conductivities, mass diffusivities, and latent heat of fusion or evaporation, are allowed to vary with the temperature and composition
- Realistic phase diagrams involving curved liquids and solidus lines are used
- Two moving boundaries are involved, i.e., the evaporative boundary and freezing boundary
- Surface temperature is determined by the combined effect of heat radiation, evaporative cooling, and thermal diffusion

Use of Computer Program

The computer program works well if the following three input program parameters are properly chosen: 1) time step size (DELT), 2) grid spacing (DELX), and 3) maximum iteration count (NIT).

PRECEDING PAGE BLANK NOT FILMED

The solidification boundary is sensitive to the grid spacing. This is because in passing through a mesh point, discontinuity in the computation occurs for the following reasons. We compute the derivatives in terms of the temperatures and concentrations at the discrete mesh points. When one mesh point is dropped because solidification occurs near it, the derivative based on a substituting new mesh point is discontinuous with that based on the previous mesh point. Though this discontinuity can be reduced by using a smaller time step size, it would be a self-defeating strategy. An alternative is to accept the discontinuous results as they occur, advantages being taken of the fact that the program corrects itself. Although the derivative dz/dt is large when the solid-liquid interface passes through a mesh point, it becomes smaller thereafter thereby correcting the solidification boundary position.

The frequency of this self-correction depends on the grid spacing. Too small a grid spacing would cause too frequent self-corrections. Too large a grid spacing, on the other hand, would obscure the rapid temperature variations around the solidification boundary. This indicates that a proper choice of the grid spacing is required to achieve an optimal tradeoff between accuracy and computing time. There is another tradeoff between the time step size and maximum iteration count for optimal computing results.

Since each evaporation-solidification problem represents a different and unique physical situation, each case must be dealt with separately. However, based on our experience, the following guidelines would be helpful:

The first consideration for the choice of the grid spacing is the behavior of the evaporation boundary after solidification begins. If the evaporation boundary is virtually stationary as

compared to the solidification boundary, the grid spacing should be chosen so that the evaporation boundary is within the first mesh interval (between the first and second mesh points). If, on the other hand, the evaporation boundary is moving at velocities comparable to those of the solidification boundary, then the grid spacing can be selected more freely. The major consideration in this case is the relationship between the grid spacing and the time step size. For a fixed time step size, the grid spacing should be chosen so that at least four time intervals (of step sizes) occur before the solidification boundary passes through a mesh point.

In cases where the evaporation boundary is virtually stationary, one must experiment to determine an optimum time step size in terms of accuracy and computing time. The conditions of the experiment are as follows. Set both the minimum time step size (DELTM) and the time printing interval (DELP) to zero. Setting the time printing interval to zero will cause the computer to print out every computer time step. Setting the minimum time step size to zero will not cause the program to cut back indefinitely but will use, as the minimum, the time step size divided by 1024. By examining the computed results, one can see at what time step sizes the program is running. By examining the actual iteration count (IT), one can see if the program is converging or not. If not converging repeatedly, a smaller time step size is indicated. If the program is converging most of the time, then the minimum time step size can be set at the level of the most frequent time step size and the actual iteration count re-examined to see if the program still converges most of the time. For long runs, the time printing interval must not be zero or small, but must be chosen in consideration with the amount of the required output.

To improve the computing time on long runs, one should consider enlarging the grid spacing as suggested above as one of the tradeoffs. In addition, one may change the maximum iteration count upwards or downwards to also improve the computing time.

Our computer program has the capability for assuming equal or unequal (doubling) mesh point spacings. Our experience, as indicated in Tables 1-4, shows that the unequal spacing scheme gives practically the same accuracy with far less computations as compared with the equal spacing scheme. This may be due to the rapidity at which the temperature declines at the evaporation boundary. Other physical situations may give different results and may indicate that the equal spacing scheme should be used.

The program input parameters consist of a set of integers IX, IAM, NIT, IM, N, and NCN; and a set of real numbers DELX, DELT, DELTM, DELP, TF, and S. IX is the maximum number of mesh points to be used in the program. Present, IX 28. IAM is the spacing option indicator. If IAM equals 0, the points of mesh are equally spaced with grid spacing DELX. If IAM = 1, an unequal spacing is indicated. The first two intervals are equal and set to DELX. Thereafter, each interval is double the previous interval in spacing. NIT is the maximum number of iterations as interpreted in the context of halving the time step size. If the step is begun at the minimum time step, the NIT is the maximum number of iterations allowed. IM is the number of mesh points in actual use. The input value of IM introduces the minimum number of mesh points to be used. Thereafter additional mesh points are added as required by a substantial change in temperature at next to last mesh point, that is, 1 degree below the initial temperature. IM is increased until IM is equal to IX.

TABLE 1 VARIATION OF TEMPERATURE (°C) AT EVAPORATIVE BOUNDARY
FOR VARIOUS COMPUTATION SCHEMES

| Scheme | I | II | III | IV | V |
|-----------------|---------------|-----------------|----------------|------------------|----------------------|
| Grid Spacing | 0.01 equal | 0.01 unequal | 0.001 equal | 0.001 unequal | 0.0001 cm unequal |
| time, ms | | | | | |
| 0.2 | 966.5 | 966.5 | 966.5 | 966.5 | 966.5 |
| 0.6 | 959.4 | 959.4 | 959.4 | 959.4 | 959.5 |
| 1.4 | 945.7 | 945.7 | 945.7 | 945.7 | 945.8 |
| 1.8 | 938.9 | 938.9 | 938.9 | 938.9 | 939.0 |
| 2.0 | 935.5 | 935.5 | 935.5 | 935.5 | 935.6 |
| 2.05 | 934.7 | 934.7 | 934.7 | 934.7 | N.C. |
| 2.075 | 934.2 | 934.2 | 934.2 | 934.2 | N.C. |
| 2.0875 | 934.0 | 934.0 | 934.0 | 934.0 | N.C. |
| 2.09375 | 933.9 | 933.9 | 933.9 | 933.9 | N.C. |
| 2.1 | 933.8 | 933.8 | 933.8 | 933.8 | 933.9 |
| 2.1125 | 933.6 | 933.6 | 933.6 | 933.6 | 933.7* |
| 2.1375 | 933.2 | 933.2 | 933.2 | 933.2 | 933.3* |
| 2.1875 | 932.4 | 932.4 | 932.4 | 932.4* | 932.5* |
| 2.2875 | 930.8 | 930.8 | 930.8 | 930.8* | 930.9* |
| 2.4875 | 927.7 | 927.7 | 927.2 | 927.7* | 927.7* |
| 2.8875 | 921.5 | 921.5 | 921.5 | 921.5* | 921.5* |
| 3.6875 | 909.3 | 909.3 | 909.3 | 909.3* | 909.3* |
| 5.2875 | 885.8 | 885.8 | 885.8 | | |

* Hand interpolations
N.C. not computed

TABLE 2 VARIATION OF POSITION (μm) OF EVAPORATIVE BOUNDARY
WITH TIME FOR VARIOUS COMPUTATION SCHEMES

| Scheme | I | II | III | IV | V |
|-----------------|---------------|-----------------|----------------|------------------|----------------------|
| Grid Spacing | 0.01 equal | 0.01 unequal | 0.001 equal | 0.001 unequal | 0.0001 cm unequal |
| time, ms | | | | | |
| 0.2 | 0.122 | 0.122 | 0.122 | 0.122 | 0.122 |
| 0.6 | 0.351 | 0.351 | 0.351 | 0.351 | 0.351 |
| 1.4 | 0.752 | 0.752 | 0.752 | 0.752 | 0.752 |
| 1.8 | 0.927 | 0.927 | 0.927 | 0.927 | 0.928 |
| 2.0 | 1.009 | 1.009 | 1.009 | 1.009 | 1.010 |
| 2.05 | 1.029 | 1.029 | 1.029 | 1.029 | N.C. |
| 2.075 | 1.039 | 1.039 | 1.039 | 1.039 | N.C. |
| 2.0875 | 1.044 | 1.044 | 1.044 | 1.044 | N.C. |
| 2.09375 | 1.046 | 1.046 | 1.047 | 1.047 | N.C. |
| 2.1 | 1.047 | 1.047 | 1.047 | 1.047 | 1.050 |
| 2.1875 | 1.048 | 1.048 | 1.048 | 1.048* | 1.052 |
| 2.2875 | 1.049 | 1.049 | 1.049 | 1.048* | 1.053 |
| 2.4875 | 1.051 | 1.051 | 1.051 | 1.050* | 1.055 |
| 2.8875 | 1.055 | 1.055 | 1.055 | 1.054* | 1.059 |
| 3.6875 | 1.061 | 1.061 | 1.062 | 1.061 | 1.066 |
| 5.2875 | 1.072 | 1.072 | 1.072 | - | - |

* Hand interpolations
N.C. not computed

TABLE 3 VARIATION OF POSITION (μm) OF SOLID-LIQUID INTERFACE

| Scheme | I | II | III | IV | V |
|--------------|---------------|-----------------|----------------|------------------|----------------------|
| Grid Spacing | 0.01 equal | 0.01 unequal | 0.001 equal | 0.001 unequal | 0.0001 cm unequal |
| time, ms | | | | | |
| 0.21 | 0.205 | 0.204 | 0.109 | 0.109 | 0.106 |
| 0.24875 | 0.211 | 0.211 | 0.179 | 0.180 | 0.408 |
| 0.28875 | 0.229 | 0.229 | 0.350 | 0.350* | 1.03 |
| 0.36875 | 0.283 | 0.283 | 0.866 | 0.860* | 2.76 |
| 0.52875 | 0.429 | 0.429 | 2.291 | N.C. | N.C. |

TABLE 4 VARIATION OF TEMPERATURE ($^{\circ}\text{C}$) AT SOLID-LIQUID INTERFACE

| Scheme | I | II | III | IV | V |
|--------------|---------------|-----------------|----------------|------------------|----------------------|
| Grid Spacing | 0.01 equal | 0.01 unequal | 0.001 equal | 0.001 unequal | 0.0001 cm unequal |
| time, ms | | | | | |
| 0.21 | 933.8 | 933.8 | 933.8 | 933.8 | 933.9 |
| 0.24875 | 927.7 | 927.7 | 927.7 | 927.7* | 927.9* |
| 0.28875 | 924.5 | 921.4 | 921.5 | 921.4* | 921.6* |
| 0.36875 | 909.3 | 909.3 | 909.3 | 909.3* | 909.4* |
| 0.52875 | 885.8 | 885.8 | 885.8 | | |

* Hand interpolations
N.C. not computed

NONCN is a nonconvergence option. Failure to converge occasionally is not necessarily an indication of unacceptable results. Therefore, it is desirable to continue computations and examine the results to see if they are acceptable. This is done by setting NONCN to 1. If NONCN is set at 0, the nonconvergent results are not printed unless called for by the print interval. If NONCN is -1, the program stops on nonconvergent results.

The quantity DELX is the grid spacing. Equal spacing and unequal double spacing both make use of this quantity as indicated in the discussion of IAM. The quantity DELT is the maximum time interval (step size) for computation. The quantity DELTM is the input minimum time interval. The program uses as its actual minimum the larger of the quantities $\text{DELT}/1024$ and DELTM. Thus, even if DELTM is set at 0, the number of halving on cutting back the time interval is at most 10 ($2^{10} = 1024$). The program in its pre-solidification phase starts with its actual time step DELTS set to $\text{DELT}/8$ and allows it to build up to DELT by quick convergence.

On the other hand, near the beginning of solidification, DELTS is allowed to cut back to as small as $\text{DELT}/256$ in order to find an acceptable start of solidification. After solidification has begun, then the restriction of DELTS is between DELTK and DELT. If halving reduces DELTS below DELTK, it is set to DELTK. The quantity DELP is the present interval. If $\text{DELP} = 0$, then every time step is printed. TPR is the time for outputting results. TPR is set originally to DELP and after printout is reset to $\text{TPR} + \text{DELP}$. The program prints results if the time TIME1 at the end of the time step equals or exceeds TPR. The program does not attempt to set DELTS so that $\text{TPR} = \text{TIME1}$. This is only a slight inconvenience when the print interval is large as compared to DELTM. Generally, we would like DELTM to be set close to the most frequent

DELTS provided that failure to converge does not ensue on a regular basis. TF is the final time of program. This means that if TIME1 equals or exceeds TF, no additional time steps are taken.

The decimal quantity S between 0 and 0.5 is used to determine closeness to a mesh point. If the boundary point (either evaporation or solidification) is such that it exceeds the point that divided the mesh interval surrounding the boundary point in the ratio $(1-S)/S$, then the mesh reference point for computation is moved to the next mesh point. The introduction of S is to make the transition due to passing a mesh point less abruptly discontinuous. The best values of S are between 0.05 and 0.15. For computations on the solid side of the solidification boundary, we continue to use the old mesh points until the boundary point passes the point that divides the new mesh interval about the solidification point in the ratio $S/(1-S)$. This strategy causes a gradual transition from one mesh point to another. The integers II1, II2 are used as reference point indicators for the solid and liquid sides, respectively. For the evaporation boundary, II3 is used to indicate which points are used. II4 is used only to indicate the first mesh point to the left of the evaporation boundary.

Typical Computer Input

The definitions of the various inputs fed into the computer are given in the Glossary of Program Parameters. Typical input values are as follows:

| | | | | |
|-------|---|----|---|-------------------------------|
| IX | = | 28 | = | maximum number of mesh points |
| IAM | = | 1 | unequal, doubled grid spacing | |
| NIT | = | 20 | maximum number of iterations | |
| IM | = | 16 | actual number of points in mesh | |
| NONCN | = | 0 | allowing the program to continue when non-convergence occurs with no special printout of these results. | |

The alloy phase diagrams are determined from the five constants ET, EA, EB, EC, and ED, which define the liquidus C_ℓ and solidus lines C_s as two functions of the temperature, T:

$$C_\ell(T) = ED \times (ET - T)^2 + EC \times (ET - T)$$

$$C_s(T) = EB \times (ET - T)^2 + EA \times (ET - T)$$

In our example of 10 mole percent ($C_o = 0.10$) of antimony in germanium initially uniform at 970°C ($T_o = 970$)

ET = melting point of pure germanium = 956°C

$$EA = 0.128812 \times 10^{-3}$$

$$EB = -0.82218 \times 10^{-7}$$

$$EC = 0.466678 \times 10^{-2}$$

$$ED = -0.60466 \times 10^{-5}$$

The evaporation constants for the solvent and solute as defined previously under "The Equation at the Evaporative Boundary" are:

$$AU = A_u = 0.1115 \times 10^2$$

$$BU = B_u = 0.863 \times 10^4$$

$$EMU = M_u = 0.2435 \times 10^3$$

$$AV = A_v = 0.1171 \times 10^2$$

$$BV = B_v = 0.1803 \times 10^5$$

$$EMV = M_v = 0.726 \times 10^2$$

$$EK = K_e = 5.833 \times 10^{-4}$$

The diffusion coefficient of the solute in solvent in the solid and liquid states are, respectively

$$DS = D_s = 0.10 \times 10^{-6}$$

$$DL = D_\ell = 0.10 \times 10^{-3}$$

The density ρ , and latent heat of evaporation, γ , of the pure solvent are, respectively,

$$\text{RHO} = \rho_v = 5.32$$

$$\text{GAMMA} = \gamma_v = 160$$

Corresponding values for pure solute are:

$$\text{RHO} = \rho_u = 6.68$$

$$\text{GAMMA} = \gamma_u = 39$$

The above give two derived quantities:

$$\text{ALS} = a_\ell^2 = k_\ell / \rho_v c$$

$$\text{ASS} = a_s^2 = k_s / \rho_v c$$

where

$$\text{CEE} = c = 0.740 \times 10^{-1} = \text{specific heat}$$

The two input parameters in the surface radiation terms are:

$$\text{EE} = \epsilon = 0.55 = \text{emissivity coefficient, and}$$

$$\text{SIG} = \sigma = 0.136 \times 10^{-7} = \text{Stefan-Boltzmann constant.}$$

Computer Output

The first line of computer outputs gives the program input parameters IX, IAM, NIT, IM, and NONCN, which are defined previously and also in the "Glossary." The next two lines of computer output give the phase diagram constants (ET, EA, EB, EC, and ED) and evaporation constants (AU, BU, EMU, AV, BV, EMV, and EK), respectively. The next printouts are for CEE, DS, DL, TO, CO, XKL, RHO, GAMMA, RHO, GAMMA, EE, SIG, T2, and COO, where T2 is the temperature when solidification begins for the melt of initial solute concentration CO.

The computed numbers are then outputted as follows:

IT = actual iteration count
IM = number of points in mesh
II1 = grid point reference for solid side of mesh
II2 = grid point reference for liquid side of mesh
II3 = grid point reference for evaporation boundary
II4 = grid point reference for point after evaporation
boundary

These printouts are then followed by the computed values associated with the evaporation boundary: time, location y , concentration C , temperature T , extent of points $X(IM)$, current time interval $DELTS$, dy/dt $DYDT1$, dC/dt $DCDT1$, dT/dt $DTDT1$. If solidification has not begun, then there is no information about the solidification boundary. Otherwise, we have position of the solidification boundary z computer language (ZI1), solid solute concentration C_s (CS1), liquid solute concentration C_ℓ (CL1), temperature T (TI1), and rate of movement dz/dt (DZDT1). All decimal outputs are five per line with excess going to the next lines.

Representative Computed Results

The study of the effect of varying the grid spacing $DELX$ on the computed results is summarized in Tables 1 through 4. The five cases considered are:

Case I: $DELX = 0.01$ cm with equal spacing
Case II: $DELX = 0.01$ cm with unequal spacing
Case III: $DELX = 0.001$ cm with equal spacing
Case IV: $DELX = 0.001$ cm with unequal spacing
Case V: $DELX = 0.0001$ cm with unequal spacing

Tables 1 and 2 indicate the insensitivity of the evaporation boundary and its temperature to grid spacing, provided that the spacing is always larger than the evaporation boundary point. Tables 3 and 4 involve solidification boundary and show that the temperature is insensitive to DELX but that the solidification boundary is quite sensitive to the choice of DELX. Thus, it is important to use DELX sufficiently small so that the solidification boundary movement is fully exhibited and not stunted by a large grid spacing relative to which the boundary size is small. The spacing affects the evaluation of the first and second temperature partial derivatives with time which are larger in absolute values for smaller spacings, due to more rapid temperature changes near the boundaries.

The figures (Figs. 2-4), prepared from the computed results in Tables 1-4, indicate the superiority of unequal over equal grid spacing. For $\text{DELX} = 0.01 \text{ cm}$, where the spacing is coarse, little difference is found in the temperature distribution. For $\text{DELX} = 0.001 \text{ cm}$, there is greater difference between the two because the equal spacing has limited the semi-infinite body to 27 (0.001 cm) and fixes the temperature at the end point to 970°C , thus not allowing the temperature to decline as rapidly as it should. For $\text{DELX} = 0.0001 \text{ cm}$, the equal spacing method could not work at all because 27 (0.0001 cm) is too small a range to define a semi-infinite body even for the small time constants under consideration.

The second set of graphs, Fig. 3 (grid spacing $\text{DELX} = 0.001$), shows wide disparity between equal and unequal spacing whereas the first set of graphs (Fig. 2) ($\text{DELX} = 0.01$) shows good agreement. The smaller DELX needs more points to simulate the semi-infinite, one dimensional case and when restricted to $\text{IX} = 28$, fails to

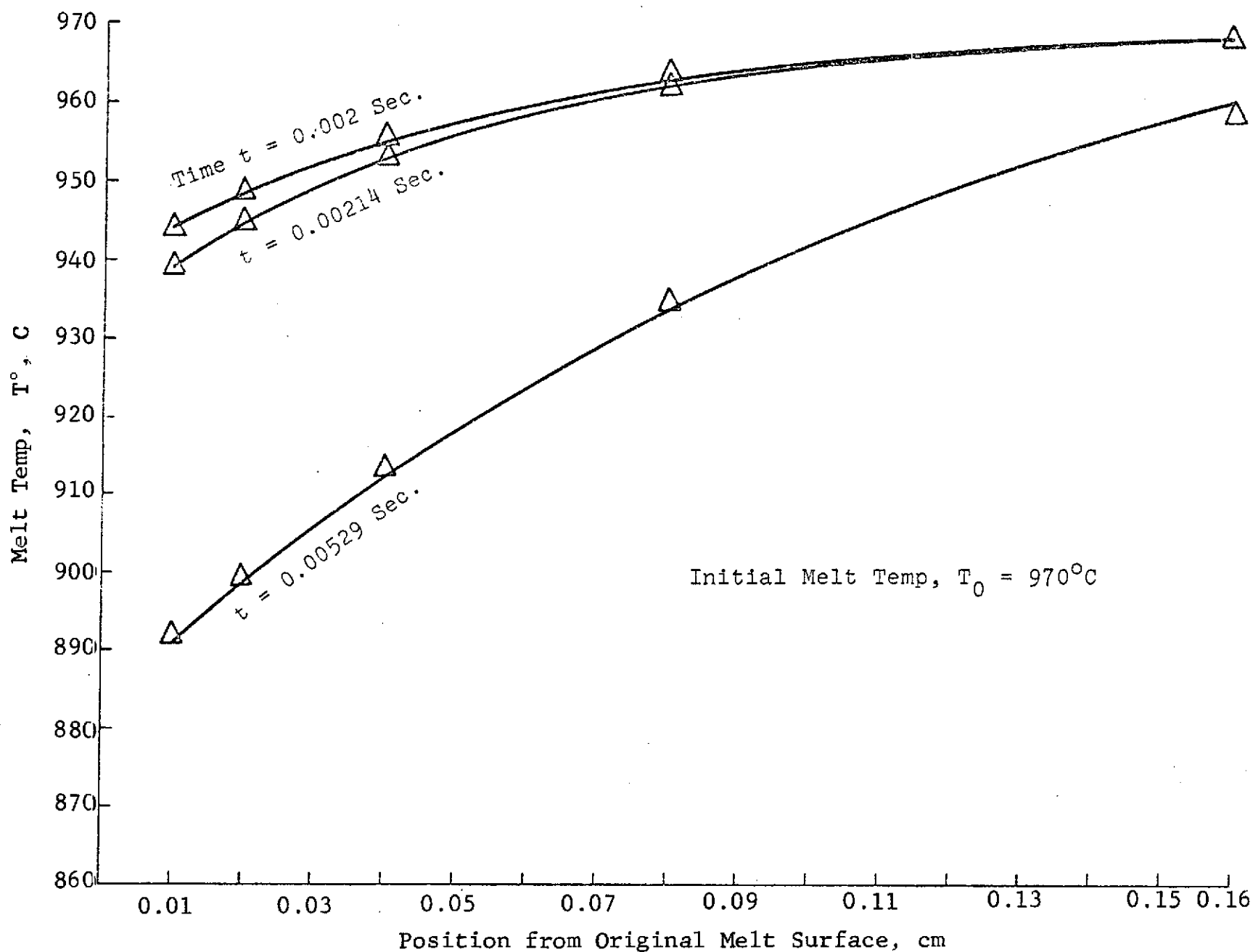


Fig. 2 Computed Temperature Distribution in Semi-infinite Body at Different Times, t (initial grid spacing = 0.01 cm)

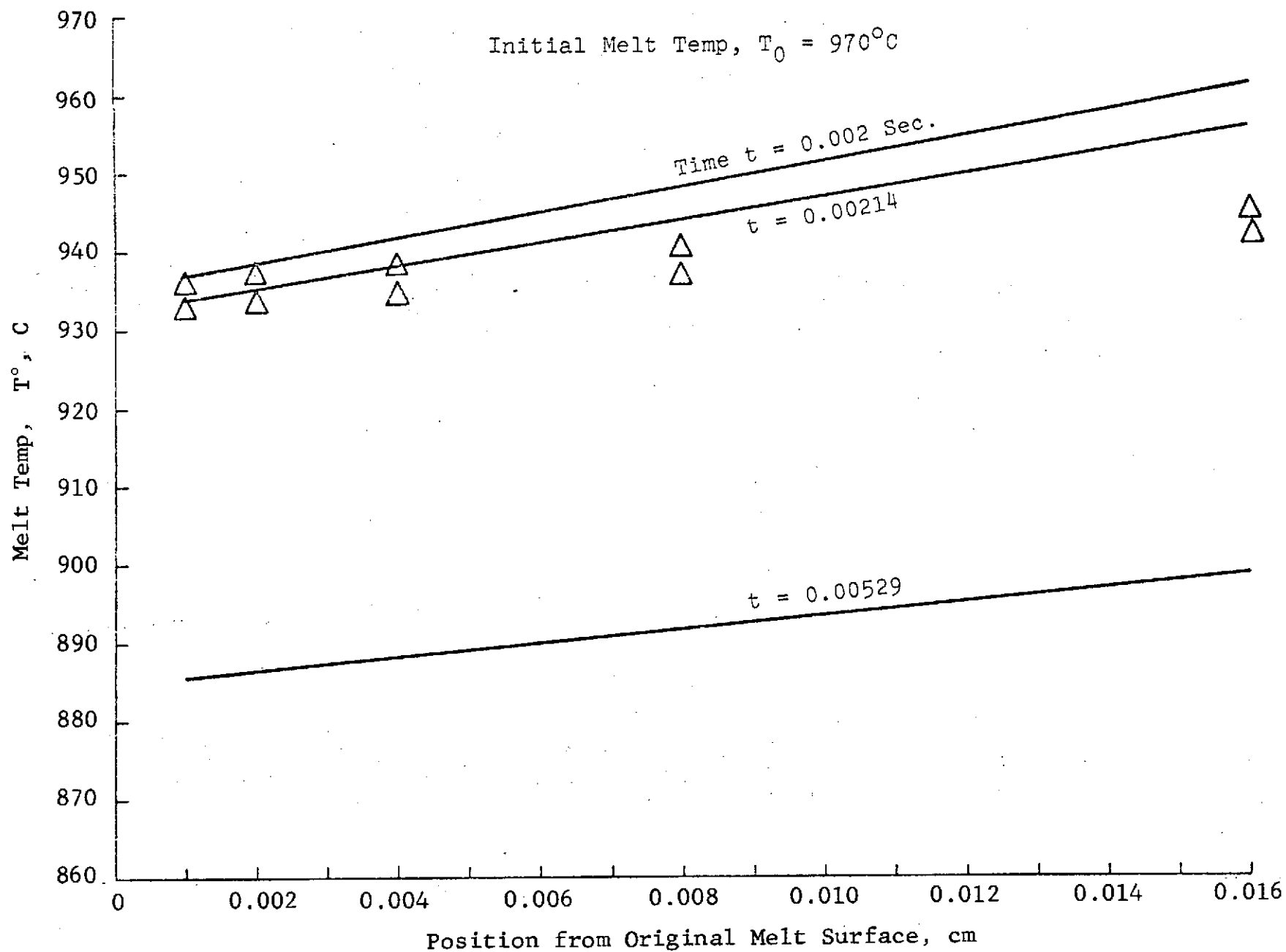


Fig. 3 Computed Temperature Distribution in the Semi-infinite Body at Different Times, t (initial grid spacing = 0.001 cm)

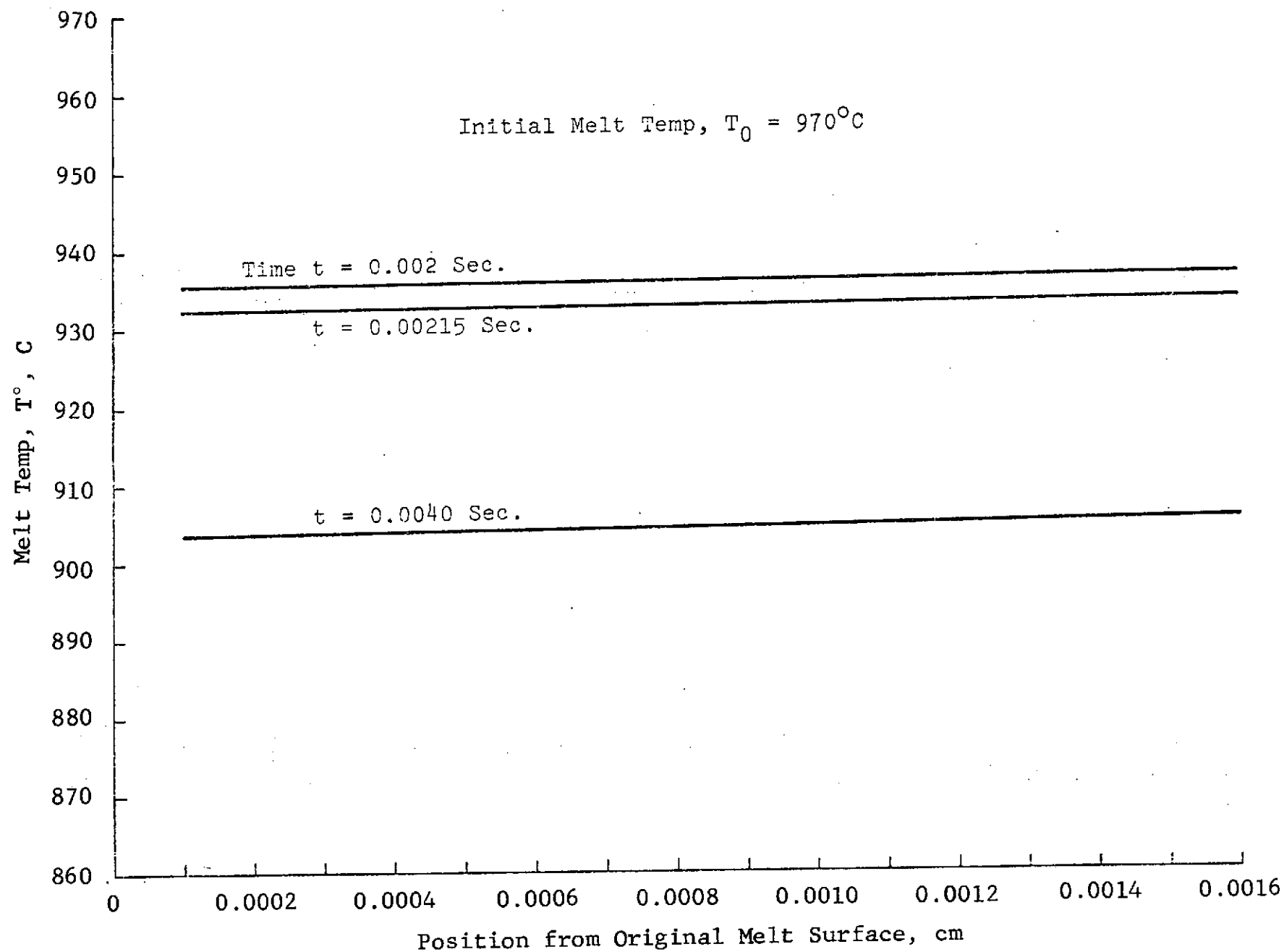


Fig. 4 Computed Temperature Distribution in Semi-infinite Body at Different Times, t (initial grid spacing = 0.0001 cm)

allow temperature away from the evaporating surface to decline rapidly because it is artificially pegged at $x = 28$ (0.001) to 970° . The unequal spacing needs but six points to give equivalent extension and, when given 10 or 11 points, can adequately span a sufficient distance to simulate semi-infinity. At smaller DELX (0.0001) one cannot even attempt to use equal spacing without modifying the behavior at the last mesh point. For unequal spacing, 16 points will adequately represent the semi-infinite body for the times under consideration.

Checking Program

To check the program, GaAs single crystals will be grown with controlled dopant type, dopant concentration, growth rate, and temperature gradient, as shown in Table 5. The dopant concentration, carrier mobilities, defect contents, ... will be measured along several sections on each crystal. The results will be statistically analyzed and presented in future reports.

TABLE 5 GaAs CRYSTAL GROWTH SCHEDULE

| Crystal No. | Dopant | Concentration | Growth Rate in./hr | Temperature Gradient °C/in. |
|-------------|---|--------------------|--------------------|-----------------------------|
| 1 | Te | 1×10^{17} | 0.16 | 8 |
| 2 | Si | 5×10^{18} | 0.22 | 8 |
| 3 | Cr | 5×10^{18} | 0.28 | 6 |
| 4 | Si | 5×10^{17} | 0.16 | 6 |
| 5 | Zn | 5×10^{18} | 0.16 | 4 |
| 6 | Cr | 1×10^{18} | 0.16 | 10 |
| 7 | Te | 1×10^{18} | 0.22 | 6 |
| 8 | Zn | 1×10^{18} | 0.28 | 8 |
| 9 | Cr | 5×10^{17} | 0.10 | 8 |
| 10 | Si | 1×10^{18} | 0.10 | 4 |
| 11 | Si | 1×10^{17} | 0.28 | 10 |
| 12 | Zn | 1×10^{17} | 0.10 | 6 |
| 13 | Te | 5×10^{17} | 0.28 | 4 |
| 14 | Zn | 5×10^{17} | 0.22 | 10 |
| 15 | Cr | 1×10^{17} | 0.22 | 4 |
| 16 | Te | 5×10^{18} | 0.10 | 10 |
| 17 | To be grown after the results of above crystals are analyzed. | | | |
| 18 | | | | |
| 19 | | | | |
| 20 | | | | |

CONCLUSIONS

We have developed a computer simulation program to study the phenomena of directional combined evaporation and solidification in binary alloys. A realistic phase diagram involving curved liquidus lines is used, and the program can be used for cases where the solid and liquid material parameters (e.g., specific heat, conductivity, diffusivity, ...) are functions of both temperature and solute concentration. The program works well if one follows the guidelines outlined in the report. The computed output results include the locations and velocities of movement of both the evaporation and solidification boundaries, and the temperature and concentration profiles in the semi-infinite alloy body at selected instants of time.

APPENDIX I
IMPROVED COMPUTER PROGRAM

PRECEDING PAGE BLANK NOT FILMED

```

      DIMENSION X(28),T(28),TT(28),C(28),CC(28),
      *TEM(10),A(84)
      NAMELIST /INVAR/CEE,DS,DL,T0,C0,XKL,RHO,GAMMA,RHOU,GAMMAU,EE,SIG
      *,ET,EA,EB,EC,ED,AU,BU,EMU,AV,BV,EMV,EK,IX
      D2(X,F,Y,G,Z,H) = ((H-G)/(Z-Y) - (F-G)/(X-Y))/(Z-X)*2.
      ABS1(X) = AMAX1(1.,ABS(X))
      UE(V) = EK*(10.** (AU-BU/(273.12+V)))/SQRT(EMU*(273.12+V))
      VE(V) = EK*(10.** (AV-BV/(273.12+V)))/SQRT(EMV*(273.12+V))
      FS(V) = (EB*(ET-V)+EA)*(ET-V)
      FL(V) = (ED*(ET-V)+EC)*(ET-V)
      XCL(V) = ET-2.*V/(EC+SQRT((EC)**2+4.*(ED)*(V)))
      XCSL(V) = ET+2.*V/((EC-EA)+SQRT((EA-EC)**2+4.*(EB-ED)*(V)))
      DFL(V) = -(2.*ED*(ET-V)+EC)
      II=1
      IO=8
      READ(II,100) IX,IAM,NIT,IM,NONCN
100  FORMAT (16I5)
      NITH=NIT/2
      NITQ=NITH/2
      NITL=NITH+NITQ
64  READ(II,101) ET,EA,EB,EC,ED
      AQUAN = -(EA-EC)**2/(4.*(EB-ED))
101  FORMAT (7E10.0)
      READ(II,101) AU,BU,EMU,AV,BV,EMV,EK
      READ(II,101) CEE,DS,DL,T0,C0,XKL,RHO,GAMMA ,RHOU,GAMMAU,EE,SIG
      ALS=XKL/(RHO*CEE)
      XKS=1.1*XKL
      ASS=1.1*ALS/1.03
      AS=SQRT(ASS)
      AL=SQRT(ALS)
      READ(II,101) DELX,DELT,DELTM,DELF,TF,S
      DELTK=AMAX1(DELTM,DELT/1024.)
      T2=XCL(CC)
      C00=FL(T2)
201  DO 1 I=1,IX
      IF(I-2) 2,3,4
      2  X(1)=0.
      GO TO 1
      3  X(2)=DELX
      GO TO 1
      4  IF(IAM) 5,5,6
      5  X(I)=X(I-1)+DELX
      GO TO 1
      6  X(I)=X(I-1)+X(I-1)
      1  CONTINUE
999  WRITE(IO,102) IX,IAM,NIT,IM,NONCN
      WRITE(IO,102) ET,EA,EB,EC,ED
      WRITE(IO,102) AU,BU,EMU,AV,BV,EMV,EK
      WRITE(IO,102) CEE,DS,DL,T0,C0,XKL,RHO,GAMMA ,RHOU,GAMMAU,EE,SIG,T2,
      *C00
      TPR=DELF
      RAT=1.
      TSI1=T0
      TI1=T0
      CSL1=C0

```

| | |
|--|----------|
| YI1=0. | BIN00560 |
| ZI1=0. | BIN00570 |
| II1=2 | BIN00580 |
| II2=2 | BIN00590 |
| II3=2 | BIN00600 |
| D2T2=0. | BIN00610 |
| D2T3=0. | BIN00620 |
| D2T4=0. | BIN00630 |
| D2C3=0. | BIN00640 |
| D2C4=0. | BIN00650 |
| D2C2=0. | BIN00660 |
| D2T1=0. | BIN00670 |
| D2C1=0. | BIN00680 |
| DTLDX=0. | BIN00690 |
| DTSDX=0. | BIN00700 |
| D2C5=0. | BIN00710 |
| D2T5=0. | BIN00720 |
| D2C6=0. | BIN00730 |
| D2T6=0. | BIN00740 |
| TIME =0. | BIN00750 |
| DCDX0=0. | BIN00760 |
| DTDY0=0. | BIN00770 |
| DELTS=DELT/8. | BIN00780 |
| TIME1=TIME+DELTS | BIN00790 |
| DO 10 I= 1,IM | BIN00800 |
| C(I)=C0 | BIN00810 |
| CC(I)=C0 | BIN00820 |
| TT(I)=T0 | BIN00830 |
| 10 T(I)=T0 | BIN00840 |
| IPL=0 | BIN00850 |
| IFS=0 | BIN00860 |
| III=II2 | BIN00870 |
| 14 IT=0 | BIN00880 |
| IF(IFS.EQ.1) GO TO 199 | BIN00890 |
| IF(IPL) 11,11,20 | BIN00900 |
| 11 U0=UP(T0) | BIN00910 |
| V0=VE(T0) | BIN00920 |
| IPL=1 | BIN00930 |
| 199 IF(IFS.NE.0) CSL1=CS1 | BIN00940 |
| IF(IFS.EQ.1) IFS=2 | BIN00950 |
| DYDT0=U0*EMU*CSL1/RHO+V0*EMV*(1.-CSL1)/RHO | BIN00960 |
| HB0=-EE*SIG*(273.12+TSI1)**4-U0*GAMMAU*CSL1-V0*GAMMA*(1.-CSL1) | BIN00970 |
| DCDT0=DCDX0*DYDT0-(U0-V0)*CSL1 | BIN00980 |
| DTDT0=DTDY0*DYDT0+HB0 | BIN00990 |
| 20 YI2=YI1+DELTS*DYDT0 | BIN01000 |
| IF(IFS.EQ.0) ZI2=YI2 | BIN01010 |
| IF(IFS.NE.0) ZI2=ZI1+DELTS*DZDT0 | BIN01020 |
| IF(ZI2.GT.X(II2+1)) ZI2=(X(II2)+YI2)/2. | BIN01030 |
| TSI2=TSI1+DELTS*DTDT0 | BIN01040 |
| TI2=TSI2 | BIN01050 |
| CSL2=CSL1+DELTS*DCDT0 | BIN01060 |
| IF(IFS.EQ.0) CL2=CSL2 | BIN01070 |
| 77 IF(IFS.EQ.0) GO TO 777 | BIN01080 |
| IF(IPL.GT.1) GO TO 877 | BIN01090 |
| III=0 | BIN01100 |

ORIGINAL PAGE IS
OF POOR QUALITY

```

877 CS2=FS(TI2)
CL2=FL(TI2)
777 D2C2=D2(ZI2,CL2,X(II2),CC(II2),X(II2+1),CC(II2+1))
CC(II2)=(CC(II2)+C(II2)+.5*DELTS*(D2C1+D2C2)*DL)/2.
CALL MOTON(X(II2),CC(II2),ZI2,CL2,X(II2+1),CC(II2+1))
IF(ZI2.LT.X(II2-1)) CC(II2-1)=CC(II2)+(X(II2-1)-X(II2))*
*(CL2-CC(II2))/(ZI2-X(II2))
IF(II1-II3-1) 83,87,84
87 XP=YI2
CP=CSL2
GO TO 184
84 XP=X(II1-2)
CP=CC(II1-2)
184 D2C4=D2(XP,CP,X(II1-1),CC(II1-1),ZI2,CS2)
CC(II1-1)=C(II1-1)+.5*DELTS*(D2C3+D2C4)*DS
CALL MOTON(X(II1-1),CC(II1-1),XP,CP,ZI2,CS2)
83 IF(II2.EQ.II1.OR.ZI2.LT.X(II2-1)) GO TO 85
IF(II2-II3.GT.1) GO TO 185
XP=YI2
CP=CSL2
GO TO 51
185 XP=X(II2-2)
CP=CC(II2-2)
51 CC(II2-1)=CP+(X(II2-1)-XP)*(CS2-CP)/
*(ZI2-XP)
85 D2T2=D2(ZI2,TI2,X(II2),TT(II2),X(II2+1),TT(II2+1))
IF(D2T2.GT.0.) D2T2=0.
TT(II2)=(TT(II2)+T(II2)+.5*DELTS*(D2T1+D2T2)*ALS)/2.
CALL MOTON(X(II2),TT(II2),ZI2,TI2,X(II2+1),TT(II2+1))
IF(IFS.EQ.0) GO TO 485
485 IF(ZI2.LT.X(II2-1)) TT(II2-1)=TT(II2)+(X(II2-1)-X(II2))*
*(TI2-TT(II2))/(ZI2-X(II2))
IF(II1-II3-1) 69,169,269
169 TP=TSI2
XP=YI2
GO TO 16
269 TP=TT(II1-2)
XP=X(II1-2)
16 D2T4=D2(XP,TP,X(II1-1),TT(II1-1),ZI2,TI2)
TT(II1-1)=T(II1-1)+.5*DELTS*(D2T3+D2T4)*ASS
CALL MOTON(X(II1-1),TT(II1-1),XP,TP,ZI2,TI2)
69 IF(II2.EQ.II1.OR.ZI2.LT.X(II2-1)) GO TO 86
52 IF(II2.LT.II3-1) GO TO 186
XP=YI2
TP=TSI2
GO TO 352
186 XP=X(II2-2)
TP=TT(II2-2)
352 TT(II2-1)=TP+(X(II2-1)-XP)*(TI2-TP)/
*(ZI2-XP)
86 IF(IFS.EQ.0) GO TO 299
DCLDX=(CL2-CC(II2))/(ZI2-X(II2))
IF(D2C2.GT.0.) DCLDX=DCLDX-D2C2*(X(II2)-ZI2)/2.
IF(D2C2.LT.0.) D2C2=0.
DTLDX=(TI2-TT(II2))/(ZI2-X(II2))

```

```

BIN01110
BIN01120
BIN01130
BIN01140
BIN01150
BIN01160
BIN01170
BIN01180
BIN01190
BIN01200
BIN01210
BIN01220
BIN01230
BIN01240
BIN01250
BIN01260
BIN01270
BIN01280
BIN01290
BIN01300
BIN01310
BIN01320
BIN01330
BIN01340
BIN01350
BIN01360
BIN01370
BIN01380
BIN01390
BIN01400
BIN01410
BIN01420
BIN01430
BIN01440
BIN01450
BIN01460
BIN01470
BIN01480
BIN01490
BIN01500
BIN01510
BIN01520
BIN01530
BIN01540
BIN01550
BIN01560
BIN01570
BIN01580
BIN01590
BIN01600
BIN01610
BIN01620
BIN01630
BIN01640
BIN01650

```



```

      IF (D2T2.LT.0.) DTLDX=DTLDX-.5*D2T2*(X(II2)-ZI2)
      IF (II3.EQ.II1) GO TO 386
      XP=X(II1-1)
      TP=TT(II1-1)
      CP=CC(II1-1)
      GO TO 486
386  XP=YI2
      TP=TSI2
      CP=CSL2
      DCSDX=(CS2-CP)/(ZI2-XP)
      DTSDX=(TI2-TP)/(ZI2-XP)
      GO TO 686
486  DCSDX=(CP-CS2)/(XP-ZI2) -D2C4*(XP-ZI2)/2.
      DTSDX=(TP-TI2)/(XP-ZI2) -D2T4*(XP-ZI2)/2.
686  DZDT=(DL*DCLDX-DS*DCSDX)/(CS2-CL2)
      DZDTT=(XKS*DTSDX-XKL*DTLDX)/(RHC*GAMMA)
      FSL=DZDT*(CS2-CL2)/DZDTT
      IF (FSL.GT.0..OR.FSL.LT.AQUAN) GO TO 772
      TII=XCSL(FSL)
      GO TO 771
772  TII=ET
771  COE1=XKS/(ZI2-XP)
      COE2=XKL/(X(II2)-ZI2)
586  TI=(RHO*GAMMA*DZDT+COE1*(TP-D2T4*.5*(XP-ZI2)**2)+COE2*(TT(II2)-.5
      **D2T2*(X(II2)-ZI2)**2))/(COE1+COE2)
773  IF (TI.LT.TSI2.AND.TI.LT.TII) TI=TII
      IF (TI.LT.TSI2.OR.TI.GT.TT(II2+1)) TI=TT(II2)
      IF (DZDT.LT.0..AND.DZDTT.GT.0.) DZDT=DZDTT
      IF (ABS(TI-TI2)-1.E-5*ABS1(TI+TI2)) 587,587,770
587  IF (ABS(DZDT-DZDT1)-1.E-3*ABS1(DZDT+DZDT1)) 298,298,770
770  TI2=(TI+TI2)/2.
      IF (DZDT.LT.0.) DZDT=DZDT1
      DZDT1=(DZDT+DZDT1)/2.
      ZI2=ZI1+.5*DELTS*(DZDT1+DZDT0)
      IF (ZI2.GT.X(II2+1)) ZI2=(X(II2)+YI2)/2.
      IIT=IIT+1
      IF (IIT.GT.5) GO TO 298
      GO TO 877
298  IF (TI.GT.TT(II2)) TI=TT(II2)
      IF (TI.LT.TSI2) TI=TSI2
      IF (II1-II3-1) 398,498,598
598  D2T6=D2(YI2,TSI2,X(II3),TT(II3),X(II3+1),TT(II3+1))
      D2C6=D2(YI2,CSL2,X(II3),CC(II3),X(II3+1),CC(II3+1))
      DTDX1=(TSI2-TT(II3))/(YI2-X(II3)) -D2T6*(X(II3)-YI2)/2.
      DCDX1=(CSL2-CC(II3))/(YI2-X(II3)) -D2C6*(X(II3)-YI2)/2.
      GO TO 599
498  DTDX1=DTSDX+D2T4*(XP-ZI2)
      DCDX1=DCSDX+D2C4*(XP-ZI2)
      D2T6=D2T4
      D2C6=D2C4
      GO TO 599
398  DCDX1=DCSDX
      DTDX1=DTSDX
      GO TO 599
299  DTDX1=(TT(II2)-TI2)/(X(II2)-YI2) -.5*D2T2*(X(II2)-YI2)

```

BIN01660
 BIN01670
 BIN01680
 BIN01690
 BIN01700
 BIN01710
 BIN01720
 BIN01730
 BIN01740
 BIN01750
 BIN01760
 BIN01770
 BIN01780
 BIN01790
 BIN01800
 BIN01810
 BIN01820
 BIN01830
 BIN01840
 BIN01850
 BIN01860
 BIN01870
 BIN01880
 BIN01890
 BIN01900
 BIN01910
 BIN01920
 BIN01930
 BIN01940
 BIN01950
 BIN01960
 BIN01970
 BIN01980
 BIN01990
 BIN02000
 BIN02010
 BIN02020
 BIN02030
 BIN02040
 BIN02050
 BIN02060
 BIN02070
 BIN02080
 BIN02090
 BIN02100
 BIN02110
 BIN02120
 BIN02130
 BIN02140
 BIN02150
 BIN02160
 BIN02170
 BIN02180
 BIN02190
 BIN02200

ORIGINAL PAGE IS
OF POOR QUALITY

```

DCDX1=(CC(II2)-CL2)/(X(II2)-YI2)-.5*D2C2*(X(II2)-YI2)
599 U1=UE(TSI2)
V1=VE(TSI2)
HB1=-EE*SIG*(273.12+TSI2)**4-U1*GAMMAU*CSL2-V1*GAMMA*(1.-CSL2)
DYDT1=U1*EMU*CSL2/RHOU+V1*EMV*(1.-CSL2)/RHO
DCDT1=DCDX1*DYDT1-(U1-V1)*CSL2
DTDT1=DTDX1*DYDT1+HB1
IF (IFL.LT.2) GO TO 76
IF (IFS.GE.1) GO TO 174
IF (TSI2.GT.TT(II2)) GO TO 399
TT2=XCL(CSL2)
IF (TSI2.GT.TT2) GO TO 174
IF (TSI2.GE.TT2-.05) GO TO 400
IF (DELTS.LE.DELTK) GO TO 400
GO TO 399
76 YI=YI1+.5*(DYDT0+DYDT1)*DELTS
IF (IFS.EQ.0) ZI=YI
TSI=TSI1+.5*(DTDT0+DTDT1)*DELTS
IF (TSI.LT.0.) TSI=TSI1
CSL=CSL1+.5*(DCDT0+DCDT1)*DELTS
IF (IFS.EQ.0) GO TO 73
IF (IIT.GT.5) GO TO 70
IF (TSI.GT.TT(II2).OR.TSI.GT.TI2) GO TO 70
73 IF (ABS(YI-YI2)-1.E-6*ABS1(YI+YI2)) 74,74,70
74 IF (ABS(CSL-CSL2)-1.E-4*ABS1(CSL+CSL2)) 75,75,70
75 IF (ABS(TSI-TSI2)-1.E-5*ABS1(TSI+TSI2)) 7,7,70
70 TSI2=(TSI+TSI2)/2.
IF (IFS.EQ.0) TI2=TSI2
YI2=(YI+YI2)/2.
IF (IFS.EQ.0) ZI2=YI2
CSL2=(CSL+CSL2)/2.
IF (IFS.EQ.0) CL2=CSL2
IF (ZI2.LT.(1.-S)*X(II2)+S*X(II2-1)) GO TO 24
22 IF (II1-II2) 24,96,96
96 II2=II2+1
46 D2C1=D2(ZI1,CL1,X(II2),C(II2),X(II2+1),C(II2+1))
D2T1=D2(ZI1,TI1,X(II2),T(II2),X(II2+1),T(II2+1))
24 IF (IT-NITQ) 48,174,160
160 IF (IT-NITH) 48,47,48
47 IF (DELTS-DELTK) 48,48,53
53 DELTS=DELTS/RAT
152 IF (RAT-1.) 153,153,154
153 RAT=2.*RAT
DELTS=DELTS/2.
GO TO 152
154 TIME1=TIME+DELTS
212 DO 45 I=II3,IM
TT(I)=(TT(I)+(RAT-1.)*T(I))/RAT
45 CC(I)=(CC(I)+(RAT-1.)*C(I))/RAT
148 RAT=1.
48 IT=IT+1
IF (IT.EQ.NITH+1) GO TO 20
IF (IT-NITL) 161,174,161
161 IF (IT-NIT) 77,77,402
402 IF (DELTS.GI.DELTK) GO TO 399

```

```

BIN02210
BIN02220
BIN02230
BIN02240
BIN02250
BIN02260
BIN02270
BIN02280
BIN02290
BIN02300
BIN02310
BIN02320
BIN02330
BIN02340
BIN02350
BIN02360
BIN02370
BIN02380
BIN02390
BIN02400
BIN02410
BIN02420
BIN02430
BIN02440
BIN02450
BIN02460
BIN02470
BIN02480
BIN02490
BIN02500
BIN02510
BIN02520
BIN02530
BIN02540
BIN02550
BIN02560
BIN02570
BIN02580
BIN02590
BIN02600
BIN02610
BIN02620
BIN02630
BIN02640
BIN02650
BIN02660
BIN02670
BIN02680
BIN02690
BIN02700
BIN02710
BIN02720
BIN02730
BIN02740
BIN02750

```

| | |
|---|----------|
| IFL=2 | BIN02760 |
| GO TO 77 | BIN02770 |
| 26 IF (NONCN) 99,48,48 | BIN02780 |
| 7 IFL=IFL+1 | BIN02790 |
| DZDT1=DZDT | BIN02800 |
| IF (IFS.NE.0) ZI2=ZI1+.5*DELTS*(DZDT0+DZDT1) | BIN02810 |
| TSI2=TSI | BIN02820 |
| YI2=YI | BIN02830 |
| IF (IFS.EQ.0) ZI2=YI2 | BIN02840 |
| CSL2=CSL | BIN02850 |
| IF (IFS.NE.0) TI2=TI | BIN02860 |
| IF (TI2.LT.TSI2) TI2=TSI2 | BIN02870 |
| IF (IFS.EQ.0) TI2=TSI2 | BIN02880 |
| IF (IFS.EQ.0) CL2=CSL2 | BIN02890 |
| GO TO 77 | BIN02900 |
| 399 IF (DELTS.LE.DELTK) GO TO 26 | BIN02910 |
| IT=NIT | BIN02920 |
| IFL=1 | BIN02930 |
| GO TO 153 | BIN02940 |
| 117 IF (TIME.EQ.TIME1) TIME1=TIME1 +DELTS | BIN02950 |
| TIME=TIME1 | BIN02960 |
| IF (RAT.NE.2..AND.RAT.NE.0.) DELTS=DELTS/RAT | BIN02970 |
| RAT=1. | BIN02980 |
| IF (IT-NITQ) 82,82,81 | BIN02990 |
| 82 IF (DELTS.GT.DELT/2.) GO TO 81 | BIN03000 |
| DELTS=DELTS+DELTS | BIN03010 |
| RAT=2. | BIN03020 |
| 81 TIME1=TIME1+DELTS | BIN03030 |
| 282 D2C1=D2C2 | BIN03040 |
| D2C3=D2C4 | BIN03050 |
| D2C5=D2C6 | BIN03060 |
| D2T3=D2T4 | BIN03070 |
| D2T1=D2T2 | BIN03080 |
| D2T5=D2T6 | BIN03090 |
| DYDT0=DYDT1 | BIN03100 |
| DCDT0=DCDT1 | BIN03110 |
| U0=U1 | BIN03120 |
| V0=V1 | BIN03130 |
| DTSDX1=DTSDX | BIN03140 |
| DCSDX1=DCSDX | BIN03150 |
| IF (IFS.NE.0) DCDX0=DCDX1 | BIN03160 |
| IF (IFS.NE.0) DTDX0=DTDY1 | BIN03170 |
| IF (IFS.NE.0) DZDT0=DZDT1 | BIN03180 |
| CSL1=CSL2 | BIN03190 |
| TSI1=TSI2 | BIN03200 |
| YI1=YI2 | BIN03210 |
| ZI1=ZI2 | BIN03220 |
| IF (IFS.NE.0) CS1=CS2 | BIN03230 |
| HB0=HB1 | BIN03240 |
| CL1=CL2 | BIN03250 |
| TI1=TI2 | BIN03260 |
| IF (YI2.LT.X (II3)) GO TO 410 | BIN03270 |
| II3=II3+1 | BIN03280 |
| D2T5=D2 (YI1, TSI1, X (II3), TT (II3), X (II3+1), TT (II3+1)) | BIN03290 |
| D2C5=D2 (YI1, CSL1, X (II3), CC (II3), X (II3+1), CC (II3+1)) | BIN03300 |

ORIGINAL PAGE IS
OF POOR QUALITY

```

410 IF (II1.EQ.II2.OR.ZI2.LT.S*X(II2)+(1.-S)*X(II2-1)) GO TO 33      BIN03310
    II1=II2                                                            BIN03320
    IF (II1-II3-1) 33,310, 110                                         BIN03330
310 XP=YI1                                                            BIN03340
    CP=CSL1                                                            BIN03350
    TP=TSI1                                                            BIN03360
    GO TO 210                                                          BIN03370
110 XP=X(II1-2)                                                        BIN03380
    CP=CC(II1-2)                                                        BIN03390
    TP=TT(II1-2)                                                        BIN03400
210 D2C3=D2(XP,CP,X(II1-1),CC(II1-1),ZI1,CL1)                        BIN03410
    D2T3=D2(XP,TP,X(II1-1),TT(II1-1),ZI1,TI1)                        BIN03420
    IF (II1-II3.NE.1) GO TO 33                                         BIN03430
    D2T5=D2T3                                                            BIN03440
    D2C5=D2C3                                                            BIN03450
    GO TO 33                                                            BIN03460
174 III=II2                                                            BIN03470
    IF (ZI2.LT.X(II2-1)) III=III-1                                     BIN03480
    IF (II1-II3.LT.2) GO TO 18                                         BIN03490
    IF (II1-II3.GT.2) GO TO 29                                         BIN03500
    TT(II3)=(T(II3)/DELTS+.5*ASS*D2T5)                                BIN03510
    *+TT(II3+1)*ASS/(X(II3+1)-X(II3))/(X(II3+1)-YI2)+TSI2*ASS/(X    BIN03520
    *(II3)-YI2)/(X(II3+1)-YI2))/(1./DELTS+ASS/(X(II3+1)-YI2)*(1./X(II3    BIN03530
    *+1)-X(II3))+1./X(II3)-YI2)))                                     BIN03540
    CC(II3)=(C(II3)/DELTS+.5*CS*D2C5)                                  BIN03550
    *+CC(II3+1)*DS/(X(II3+1)-X(II3))/(X(II3+1)-YI2)+CSL2*DS/(X(I    BIN03560
    *I3)-YI2)/(X(II3+1)-YI2))/(1./DELTS+DS/(X(II3+1)-YI2)*(1./X(II3+1)    BIN03570
    *-X(II3))+1./X(II3)-YI2)))                                         BIN03580
    GO TO 18                                                            BIN03590
29 X(II3-1)=(YI2+YI1)/2.                                              BIN03600
    C(II3-1)=CSL1                                                       BIN03610
    CC(II3-1)=CSL2                                                       BIN03620
    T(II3-1)=TSI1                                                       BIN03630
    TT(II3-1)=TSI2                                                       BIN03640
    CALL TRISI(X,T,TT,II3-1,III-1,ASS,DELTS,A)                        BIN03650
    CALL TRIST(X,C,CC,II3-1,III-1,DS,DELTS,A)                        BIN03660
    GO TO 18                                                            BIN03670
27 IF (T(IM-1)-T0+1.E0) 30,32,32                                     BIN03680
30 IF (IM-IX) 15,32,32                                                 BIN03690
15 IM=IM+1                                                            BIN03700
    T(IM)=TC                                                            BIN03710
    C(IM)=CO                                                            BIN03720
32 TT(IM)=T(IM)                                                        BIN03730
    CC(IM)=C(IM)                                                        BIN03740
    GO TO 14                                                            BIN03750
18 IF (DELTS.LT.DELTK) DELTS=DELTK                                    BIN03760
    CALL TRIST(X,T,TT,III,IM,ALS,DELTS,A)                             BIN03770
    CALL TRIST(X,C,CC,III,IM, DL,DELTS,A)                             BIN03780
    DO 21 I=II2,IM                                                     BIN03790
    IF (I.EQ.II2) GO TO 21                                             BIN03800
21 CONTINUE                                                            BIN03810
219 IF (IPL.EQ.2) GO TO 117                                           BIN03820
    GO TO 48                                                            BIN03830
33 IF (TIME -TPR) 50,34,34                                            BIN03840
50 IF (NONCN) 98,98,54                                                BIN03850

```

| | | |
|-----|--|----------|
| 54 | IF (IT-NIT) 98,98,42 | BIN03860 |
| 34 | IF (DELP.EQ.C.) GO TO 42 | BIN03870 |
| | TPR=TPR+DELP | BIN03880 |
| 42 | WRITE (IO,100) IT,IM,II1,II2,II3 | BIN03890 |
| | WRITE (IO,102) TIME,YI1,CS1,TSI1,U1,V1,HB1,DYDT1,DTDT1,DCET1,DELTS | BIN03900 |
| | IF (IFS.NE.0) WRITE (IO,102) ZI1,CS1,CL1,TI1,DZDT1 | BIN03910 |
| 143 | WRITE (IO,102) (TT(I),I=II3,IM), (CC(I),I=II3,IM) | BIN03920 |
| 102 | FORMAT (5E14.6) | BIN03930 |
| | IF (TIME -TF) 98,99,99 | BIN03940 |
| 98 | DO 97 I=II3,IM | BIN03950 |
| | TTT=TT(I)+RAT*(TT(I)-T(I)) | BIN03960 |
| | T(I)=TT(I) | BIN03970 |
| | TI(I)=TTT | BIN03980 |
| 97 | CONTINUE | BIN03990 |
| | DO 197 I=II3,IM | BIN04000 |
| | CCC=CC(I)+RAT*(CC(I)-C(I)) | BIN04010 |
| | C(I)=CC(I) | BIN04020 |
| 197 | CC(I)=CCC | BIN04030 |
| | IFL=1 | BIN04040 |
| | GO TO 27 | BIN04050 |
| 400 | CSS=PS(TI2) | BIN04060 |
| | CLL=PL(TI2) | BIN04070 |
| | DELZ=(CLL-CL2)/((CLL+CC(II2))-2.*CSS)*(X(II2)-YI2) | BIN04080 |
| | ZI2=YI2+DELZ | BIN04090 |
| | DZDT=DELZ/DELTS | BIN04100 |
| | DZDT1=DZDT0 | BIN04110 |
| | CL2=CLL | BIN04120 |
| | CS2=CSS | BIN04130 |
| | DCDX0=0. | BIN04140 |
| | DTDX0=0. | BIN04150 |
| | DTDX1=0. | BIN04160 |
| | WRITE (IO,103) TIME1,YI2,TI2,ZI2,CS2,CL2,DELZ,DELTS,DZDT0 | BIN04170 |
| 103 | FORMAT(' SOLIDIFICATION HAS BEGUN '/(5E14.6)) | BIN04180 |
| | IFS=1 | BIN04190 |
| | GO TO 174 | BIN04200 |
| 99 | READ (II,INVAR) | BIN04210 |
| | IF (IX.GT.0) GO TO 999 | BIN04220 |
| | STOP | BIN04230 |
| | END | BIN04240 |

ORIGINAL PAGE IS
OF POOR QUALITY

APPENDIX II

GLOSSARY OF PROGRAM PARAMETERS

| | |
|-------|---|
| IX | = maximum number of points in mesh, ≤ 28 |
| IAM | = spacing option: 0 indicates equal, 1 unequal doubling |
| NIT | = maximum iteration count |
| IM | = number of points in mesh |
| NONCN | = nonconvergence option: 1 indicates proceed and printout 0 indicates proceed but do not printout -1 indicates program stop |
| IT | = actual iteration count |
| NITH | = half of NIT |
| NITQ | = quarter of NIT |
| NITL | = $3/4$ NIT |
| IFL | = indicator of convergence: 2 on convergence, < 2 before convergence |
| IFS | = indicator of beginning of solidification: IFS = 0 before solidification, IFS > 0 after solidification |
| II1 | = grid point reference for solid side of mesh |
| II2 | = grid point reference for liquid side of mesh |
| II3 | = grid point reference for evaporation boundary |
| II4 | = grid point reference for point after evaporation boundary |
| III | = grid point reference for point after solidification boundary |
| DELT | = maximum time interval (step size) |
| DELTM | = minimum time interval |
| DELTK | = larger of quantities DELT/1024 and DELTM |
| DELTS | = current time interval |
| TIME | = time at beginning of time interval |
| TIME1 | = time at end of time interval |
| DELP | = time print interval |
| TPR | = time for printing results |
| TF | = final time |

PRECEDING PAGE BLANK NOT FILMED

| | |
|---------------------------|---|
| YI, YI1, YI2 | = values of y (evaporation boundary) |
| ZI1, ZI2 | = values of z (solid-liquid boundary) |
| TI, TII, TI1, TI2 | = temperatures at solid-liquid boundary |
| TSI, TSI1, TSI2 | = temperatures at evaporation boundary |
| CSL, CSL1, CSL2 | = concentration at evaporation boundary |
| CS1, CS2 | = concentration of solid at solid-liquid boundary |
| CL1, CL2 | = concentration of liquid at solid-liquid boundary |
| DZDT, DZDTT, DZDT0, DZDT1 | = $\frac{dz}{dt}$ derivative of solid-liquid boundary |
| DYDT0, DYDT1 | = $\frac{dy}{dt}$ derivative of evaporation boundary |
| DTDT0, DTDT1 | = $\frac{dT}{dt}$ derivative of temperature at evaporation boundary |
| DCDT0, DCDT1 | = $\frac{dC}{dT}$ derivative of concentration at evaporation boundary |
| DTDX0, DTDX1 | = $\left(\frac{\partial T}{\partial x}\right)_y$ partial derivative for temperature at evaporation boundary |
| DTSDX | = $\left(\frac{\partial T_s}{\partial x}\right)_z$ partial derivative of temperature in solid at boundary |
| DTL DX | = $\left(\frac{\partial T_L}{\partial x}\right)_z$ partial derivative of temperature in liquid at boundary |
| DCDX0, DCDX1 | = $\left(\frac{\partial C}{\partial x}\right)_y$ partial derivative of concentration at evaporation boundary |
| DCSDX | = $\left(\frac{\partial C_s}{\partial x}\right)_z$ partial derivative of concentration in solid at solid-liquid boundary |
| DCLDX | = $\left(\frac{\partial C_L}{\partial x}\right)_z$ partial derivative of concentration in liquid at solid-liquid boundary |

| | |
|--------------------|--|
| D2T1, D2T2 | $= \left(\frac{\partial^2 T_2}{\partial x^2} \right)_z$ at liquid side of solid-liquid boundary |
| D2T3, D2T4 | $= \left(\frac{\partial^2 T_s}{\partial x^2} \right)_z$ at solid side of solid-liquid boundary |
| D2T5, D2T6 | $= \left(\frac{\partial^2 T}{\partial x^2} \right)_y$ at evaporation boundary |
| D2C1, D2C2 | $= \left(\frac{\partial^2 c_2}{\partial x^2} \right)_z$ at liquid side of solid-liquid boundary |
| D2C3, D2C4 | $= \left(\frac{\partial^2 c_s}{\partial x^2} \right)_z$ at liquid side of solid-liquid boundary |
| D2C3, D2C4 | $= \left(\frac{\partial^2 c_s}{\partial x^2} \right)_z$ at solid side of solid-liquid boundary |
| D2C5, D2C6 | $= \left(\frac{\partial^2 c}{\partial x^2} \right)_y$ at evaporation boundary |
| U0, U1 | = rates of evaporation of solute |
| VO, V1 | = rates of evaporation of solvent |
| HBO, HBI | = heat balance sum of evaporation and radiation terms |
| EMU, EMV | = molecular weight of solute and solvent atoms |
| RHO, RHO | = density of solute and solvent |
| GAMMA, GAMMA | = specific heats of solute and solvent |
| AU, BU, AV, BV, EK | = evaporation constants for solute and solvent |
| UE, VE | = arithmetic function definition for evaporation rates |
| ET, EA, EB, EC, ED | = phase diagram constants |
| FS, FL | = arithmetic functions for solidus and liquidus curves |

| | |
|----------|--|
| AS, AL | = temperature diffusion coefficients |
| ASS, ALS | = squares of temperature diffusion coefficients |
| XKS, XKL | = k_s, k_ℓ for interphase boundary equation |
| DS, DL | = mass (concentration) diffusion coefficient |
| EE, SIG | = radiation constants ϵ, σ |
| TO, CO | = initial temperature and concentration distribution |
| COO | = equals CO |

APPENDIX III

LIST OF SYMBOLS

| | |
|------------|---|
| A_ℓ | $k_\ell/\rho_v c$ |
| A_s | $k_s/\rho_v c$ |
| A_u, B_u | evaporating constants for solute |
| A_v, B_v | evaporating constants for solvent |
| c | specific heat, cal/g/°C |
| C | solute concentration |
| C_ℓ | solute concentration in liquid |
| C_o | initial solute concentration in liquid |
| C_s | solute concentration in solid |
| D_s | density of solid, g/cm ³ |
| D_ℓ | density of liquid, g/cm ³ |
| E_T | melting point of solvent, °C |
| E_A, E_B | coefficients of solidus |
| E_C, E_D | coefficients of liquidus |
| f_ℓ | liquidus equation |
| f_s | solidus equation |
| K_e | constant in evaporation equations = 5.83×10^{-5} |
| k_ℓ | thermal conductivity of liquid, cal/sq cm/cm/sec/°C |
| k_s | thermal conductivity of solid, cal/sq cm/cm/sec/°C |
| M_u | molecular weight of solute |
| M_v | molecular weight of solvent |

| | |
|------------|--|
| S | time constant |
| t | time, second |
| T | temperature, °C |
| T_i | temperature at solid-liquid interface, °C |
| T_ℓ | temperature in liquid, °C |
| T_o | initial melt temperature, °C |
| T_s | temperature in solid, or surface temperature, °C |
| T_1 | surface temperature, °C |
| T_2 | final surface temperature, °C |
| U | solute evaporating rate, $\text{mol}/\text{cm}^2/\text{sec}$ |
| V | solvent evaporating rate, $\text{mol}/\text{cm}^2/\text{sec}$ |
| v | position and temperature-dependent variable |
| x | distance from initial melt surface, cm |
| y | distance at phase change boundary, cm |
| \dot{y} | rate of movement of phase change boundary, cm/sec |
| z | distance at phase change boundary, cm |
| α | constant |
| ϵ | emissivity coefficient |
| ρ | density, g/cm^3 |
| ρ_u | density of solute, g/cm^3 |
| ρ_v | density of solvent, g/cm^3 |
| γ | latent heat of fusion, cal/g |
| γ_u | latent heat of fusion, or specific heat, of solute, cal/g or $\text{cal}/\text{g}/^\circ\text{C}$ |
| γ_v | latent heat of fusion, or specific heat, of solvent, cal/g or $\text{cal}/\text{g}/^\circ\text{C}$ |
| σ | Stefan-Boltzmann constant = 1.35×10^{-6} |

REFERENCES

1. Li, C. H., Phys. Stat. Solidi 15, 3 and 419, 1966.
2. Li, C. H., "Review of Grumman Studies in Metal Solidification," Grumman Research Memorandum RM-525, 1971.
3. Li, C. H., Final Report, NASA Contract NAS 8-27891, Grumman Research Report RE-458, June 1972.
4. Mukerjee, J. L., Gupta, K. P., and Li, C. H., "Evaporative Segregation in 80%-20% Cr and 60%-40% Ni Alloys," Grumman Research Memorandum RM-552, October 1972; J. Vac. Sci. 11, 33, 1974
5. Mukerjee, J. L., Gupta, K. P., and Li, C. H., "Purification Kinetics of Beryllium during Vacuum Induction Melting," Grumman Research Memorandum RM-553, 1971.
6. Zinsmeister, G., Vakuum-Tech., No. 8, 223, 1964.
7. Li, C. H., "Evaporation in Space Processing," AIAA meeting, Boston, July 1974.
8. Reichman, J., "Solidification of Metal Spheres in Vacuum," Grumman Research Memorandum RM-544, June 1972.
9. Chalmers, B., Solidification, Wiley, New York, 1969.
10. Tillier, W., "Solidification" in Physical Metallurgy, Ed. R. W. Cahn, Wiley, New York, 1965, pp. 385-441.
11. Christian, J. W., The Theory of Transformations in Metals and Alloys, Pergamon Press, New York, 1965, pp. 527-593.
12. Li, C. H., "Solidification," to be published in Materials Science Series, Academic Press, New York, 1975.
13. Rubenstein, L. I., The Stefan Problem, Amer. Math. Soc., Providence, Rhode Island, 1971.
14. Li, C. H., Progress Report No. 2 under NASA Contract NAS 8-27891, March 1972.
15. Dushman, S., Scientific Foundations of Vacuum Techniques, Wiley, New York, 1962.